5-2014

Dissecting the Function of Ack Family Kinases in Drosophila Through Understanding Their Interactions with Dock and CDC42

Abbas M. Abdallah
Purdue University

Graduate School ETD Form 9
(Revised 01/14)

PURDUE UNIVERSITY
GRADUATE SCHOOL
Thesis/Dissertation Acceptance

This is to certify that the thesis/dissertation prepared

By Abbas Mohamad Ali Abdallah

Entitled
DISSECTING THE FUNCTION OF ACK FAMILY KINASES IN DROSOPHILA THROUGH UNDERSTANDING THEIR INTERACTIONS WITH DOCK AND CDC42

For the degree of Doctor of Philosophy

Is approved by the final examining committee:

Donald Ready

Claudio Aguilar

Henry C. Chang

James Clemens

To the best of my knowledge and as understood by the student in the *Thesis/Dissertation Agreement. Publication Delay, and Certification/Disclaimer (Graduate School Form 32)*, this thesis/dissertation adheres to the provisions of Purdue University's "Policy on Integrity in Research" and the use of copyrighted material.

Henry C. Chang

Approved by Major Professor(s): _____

_____

Approved by: Peter J. Hollenbeck 04/24/2014

Head of the Department Graduate Program Date

DISSECTING THE FUNCTION OF ACK FAMILY KINASES IN *DROSOPHILA* THROUGH UNDERSTANDING THEIR INTERACTIONS WITH DOCK AND CDC42

A Dissertation

Submitted to the Faculty

of

Purdue University

by

Abbas M. Abdallah

In Partial Fulfillment of the

Requirements for the Degree

of

Doctor of Philosophy

May 2014

Purdue University

West Lafayette, Indiana

To my family and friends, especially my mom and dad for all the sacrifices they have made to make this day possible. I am forever grateful and would have never have been able to do it without you. To my grandma for her endless love and prayers. To my wife, the love of my life. The woman who always stood by my side, always believed in me and never let go.

ACKNOWLEDGEMENTS

I would like to thank my committee members: Dr. Donald Ready for his great support and advice regarding not only science, but career path and future plans. Dr. James Clemens for helping me learn several techniques, collaborating on several experiments with us, and giving crucial feedback to our work. Dr. Claudio Aguilar for being an excellent mentor. His endless contribution and feedback to my ideas during our joint lab meetings over the years were extremely important to the advancement of my project and to my growth as a scientist. Combined they have helped me maneuver my way through the rocky PhD path. I would also like to thank my former lab mate Xin Zhou for his help in certain experimental procedures. Also I would like to thank several undergrads who have contributed to my work especially Christine Kim, Kushani Shah, and Christopher Hogden, Finally my Special thanks to my Advisor Dr. Henry Chang for his endless help, support, and guidance during my project. He has been a true mentor on many levels and helped greatly in shaping my career path. I especially enjoyed the luxury of being able to discuss experiments and ideas with on a daily basis anytime. Thank you for all the hard work you have done for me whether theoretical or on bench.

TABLE OF CONTENTS

Page

LIST OF FIGURES viii

ABSTRACT x

CHAPTER 1. INTRODUCTION 1

1.1 Tyrosine phosphorylation: identification and significance 1

1.2 Non receptor tyrosine kinases 2

1.3 Ack is a non-receptor tyrosine kinase 3

1.4 Ack domain organization and function 4

1.5 Ack binds to activated Cdc42, a key regulator for actin cytoskeleton 5

1.6 Ack may play a role in clathrin dependent endocytosis 5

1.7 Ack in cancer 6

CHAPTER 2. MATERIALS AND METHODS 8

2.1 Fly genetics and molecular biology 8

2.2 Antibody and immunofluorescence microscopy 9

2.3 Quantification of elongated germ cell cysts 10

2.4 Quantitative RT-PCR 10

2.5 Co-immunoprecipitation and western analysis 11

2.6 Cytokinesis defect quantification 13

Page

CHAPTER 3. ACK RECRUITS DOCK TO PROMOTE *DROSOPHILA* SPERMATOGENESIS 14

3.1 Loss of Ack disrupts sperm formation in *Drosophila* males 14

3.2 *Drosophila* spermatogeneis 14

3.3 Disruption of *Ack* function prevents the formation of mature sperms. 15

3.4 Ack^{86} spermatids fail to coil properly. 16

3.5 Ack is required cell autonomously for spermatogenesis. 17

3.6 Mouse ACK1 can functionally substitute for Ack. 19

3.7 The SAM, SH3, and kinase domains are indispensable for Ack function in male fertility. 19

3.8 Ack associaes with peripheral clathrin positive structures 20

3.9 The SAM and SH3 domains are critical for Ack subcellular localization 22

3.10 Ack is required for Dock localization in male germ cells. 24

3.11 Dock SH2 is essential for localization in male germ cells. 25

CHAPTER 4. PR2 REDUCES ACTIVATED CDC42 CYTOKINESIS DEFECT 27

4.1 Expression of dominant active Cdc42 in male germ cells disrupts cytokinesis 27

4.2 Expression of dominant active Cdc42 in male germ cells disrupts spermatogenesis 28

4.3 Dominant active Cdc42 disrupts cytokinesis 29

Page

4.4 Expression of dominant active Rac and Rho1 in male germ cells does not affect cytokinesis 30

4.5 Constitutively activate mutation alter the subcellular localization of Cdc42 31

4.6 Cdc42-positive aberrant structures contain elevated level of phosphotyrosine 32

4.7 *PR2* suppresses Cdc42-dependent cytokinesis defect 33

4.8 $Cdc42^{G12V}$ recruits PR2 34

CHAPTER 5. DISCUSSION 37

5.1 Ack is required for proper sperm formation 37

5.2 Ack and PR2 are not redundant 38

5.3 Ack doesn't impact the apoptotic machinery in spermatogenesis 39

5.4 Ack associates with clathrin positive structures 39

5.5 SAM and SH3 contribute to Ack proper localization 41

5.6 Proper Dock localization in germ cells is dependent on Ack 42

5.7 Ack recruits Dock and potentially WASp to promote *Drosophila* spermatogenesis 44

5.8 Over-expression of $Cdc42^{G12V}$ causes cytokinesis defects in germ cells 44

5.9 $Cdc42^{G12V}$ is recruited to the contractile rings 45

5.10 $Cdc42^{G12V}$ recruits PR2 45

Page

5.11 Loss of PR2 reduces the cytokinesis defect 46

5.12 Ack and PR2 in disease..... 47

REFERENCES 66

VITA 73

LIST OF FIGURES

Figure Page

Figure 1. Ack is required for spermatogenesis……..48

Figure 2. The requirement of Ack function in spermatogenesis is cell autonomous……...51

Figure 3. Ack function in spermatogenesis requires SAM, tyrosine kinase, and SH3…….....……52

Figure 4. Ack is localized to endocytic clathrin structures inspermatocyte……...53

Figure 5. Ack localization requires SAM and SH3……....54

Figure 6. Dock localization requires Ack…….55

Figure 7. Dock localization requires the SH2 domain. ……56

Figure 8. Exogenously expressed Ack and PR2 show few overlaps in spermatocytes……57

Figure 9. Endogenous Ack are seen as vesicular structures around cell periphery……..……..57

Figure 10. Dock localizes to the ring canals in spermatocytes:……..58

Figure 11. Over-expression of activated Cdc42 causes cytokinesis defect…… 59

Figure 12. Over-expression of dominant negative dRho1 causes cytokinesis defect:……60

Figure 13. Activation of Cdc42 alters its subcellular localization:……...61

Figure 14. Activated Cdc42 disrupts contractile ring……...62

Figure 15. PR2 loss of function reduces the cytokinesis defect caused by $Cdc42^{G12V}$……....63

Figure Page

Figure 16. Cdc42^{G12V} alters the localization of Ack and PR2…….. 64

Figure 17. PR2 is pulled down in complex with Cdc42^{G12V}…….. 65

ABSTRACT

Abdallah, Abbas M. Ph.D., Purdue University, May 2014. Understanding the function of Ack family kinases in *Drosophila* through dissecting their interactions with Dock and Cdc42. Major Professor: Henry Chang.

Deregulation of Ack (Activated Cdc42-associated Kinase) family of non-receptor tyrosine kinases in mammals correlates with poor prognosis in cancers and has been implicated in promoting metastasis. In Drosophila, Ack family is constituted of two kinases: Ack and PR2. To further understand the in vivo function of this family we have conducted two projects:

First we , we characterized the developmental defects of a null mutation in Drosophila Ack, which bears a high degree of sequence similarity to mammalian ACK1 but lacks a CRIB domain. We show that Ack, while not essential for viability, is critical for sperm formation. This function depends on Ack tyrosine kinase activity and is required cell autonomously in differentiating male germ cells at or after the spermatocyte stage. Ack associates predominantly with endocytic clathrin sites in spermatocytes, but disruption of Ack function has no apparent effect on clathrin localization and receptor-mediated internalization of Boss (Bride of sevenless) protein in eye discs. Instead, Ack is required for the subcellular distribution of Dock (dreadlocks), the Drosophila homolog of the SH2- and SH3-containing adapter protein Nck. Moreover, Dock forms a complex with

Ack, and the localization of Dock in male germ cells depends on its SH2 domain. Together, our results suggest that Ack-dependent tyrosine phosphorylation recruits Dock to promote sperm differentiation.

Second, despite the fact that ACK1 has been originally identified by its ability to bind to activated Cdc42, the physiological relevance of this binding has not been described. To test the significance of this interaction, we have established an over-expression system of various Cdc42 constructs in Drosophila germ cells. Similar to Drosophila embryos, expression of constitutively active Cdc42 ($Cdc42^{G12V}$) in Drosophila spermatocytes results in cytokinesis defects, suggesting the step(s) affected by excessive Cdc42 activity is both meiotic and mitotic. $Cdc42^{G12V}$ is recruited to the site of cytokinesis ring constriction in germ cells where an increase in the level of tyrosine phosphorylation is also observed. This implies that a tyrosine kinase/substrate responds to Cdc42 activation. Indeed, loss-of-function mutations in PR2 but not Ack suppresses $Cdc42^{G12V}$-dependent cytokinesis defect, suggesting that PR2 acts downstream of Cdc42. Moreover, PR2 is co-IPed with activated Cdc42 but not wild type Cdc42. Finally we show that $Cdc42^{G12V}$ alters the subcellular localization of PR2 recruiting it to the site of cellular division.

CHAPTER 1. INTRODUCTION

1.1 Tyrosine phosphorylation: identification and significance

In 1979, during their work on polyomavirus middle T and v-Src associated kinase, Tony Hunter and two of his colleagues (Walter Eckhart and Mary Anne Hutchinson) were the first to discover that phosphate is capable of attaching to tyrosine (Eckhart et al., 1979). Soon after, Ushiro and Cohen were able to establish the importance of tyrosine phosphorylation in intracellular processes and revealed that changes in protein kinase activity occur in mammalian cells (Ushiro & Cohen 1980). Thirty five years later, our understanding of tyrosine phosphorylation and its impact on many cellular processes has tremendously increased.

Tyrosine phosphorylation occurs when a phosphate group from an ATP gets added to a tyrosine residue on substrate protein, generally by a protein tyrosine kinase. Despite the fact that tyrosine phosphorylation is estimated to account for only 1% of all phosphorylated events in human cells (Olsen et al., 2006), it can serve a wide variety of functions ranging altering enzymatic activity to creating a binding site for other proteins. Indeed, a key step in tyrosine phosphorylation dependent signaling is the ability of SH2 domain to recognize and bind phosphor-tyrosine residues (Pawson, 2004). SH2 containing proteins,

on the other hand, can be adaptor proteins capable of recruiting other signaling proteins, enzymes acting on substrate molecules, cytoplasmic tyrosine kinases adept of signal relay, E3 ubiquitin ligases, and transcription factors (Hunter, 2009).

Over the past years tyrosine phosphorylation proved to be involved in several cellular processes such as growth factor receptor signaling (Schlessinger & Ullrich, 1992), cell adhesion via integrin signaling (lin et al., 1994) , metabolic regulation through insulin, cell cycle control through CDKS inhibition (reviewed in Lew & Kornbluth 1996), neuronal transmission (reviewed in Boxall and Lancaster 1998) and even aging. This diversity and importance of tyrsoine phosphorylation suggests that tight regulation is required to maintain normal cellular function. Indeed deregulation of tyrosine phosphorylation has been implicated in many human diseases and cancers.

1.2 Non receptor tyrosine kinases

Tyrosine kinases are divided into two categories: transmembrane Receptor tyrosine Kinases (RTK) and Non-receptor tyrosine Kinases (NTK). RTKs are generally composed of an extracellular ligand binding domain, a transmembrane domain and a cytosolic domain. While NTK are mostly cytosolic, some can associate with plasma membrane after post translational modifications such as myristoylation. In addition to the kinase domain, the NTKs may possess several domains that mediate protein-protein, protein lipid, and/or protein DNA interactions. For example, Src homology two (SH2) domain can bind to

phosphotyrosine (PY) residues while Src Homology three (SH3) domain can bind to proline rich regions. Additionally, Plakstrin homology (PH) domain is known to bind specifically phosphorylated phosphatidylinositol lipids (Isakoff et al., 1998).

Thus far, ten different families of NTKs that differ in domain organization have been identified. While the kinase domain is universal among all families and few domains are found in more than one family (such as SH3, SH2, and integrin binding domain (FERM)), several domains are family specific. DNA and actin binding domains are only present in Abl family, CIP4 homology domain is only present in Fes family, and Cdc42-Rac interactive binding domain (CRIB) is only present in Ack. Moreover, while the function of several of these domains has been identified, some remain to be elucidated. Indeed, despite the fact that Ack was originally identified by its ability to bind to GTP-bound Cdc42 (Activated Cdc42-associated Kinase), the significance and the physiological role of this binding -if any- remains poorly understood.

1.3 Ack is a non-receptor tyrosine kinase

ACK1 (activated Cdc42 kinase), a non-receptor tyrosine kinase identified by its ability to interact with GTP-bound Cdc42 (Manser et al., 1993), has been implicated in diverse cellular functions, including survival, proliferation, and migration (Eisenmann et al., 1999; Galisteo et al., 2006; Yang et al., 1999). Mammals have two ACK1-related genes, ACK1 and TNK1 (also known as TNK2 and Kos1, respectively) that differ in domain organization. ACK1 has a CRIB domain while TNK1 doesn't. *Drosophila* also has two Ack related genes: dAck

(lacks the CRIB domain) and dPR2 (has a CRIB. For simplicity, we will refer to them as Ack and PR2 hereafter). Ack was identified when co-purified in complex with other proteins capable of binding Dock's SH2 domain in S2 cell lysates (Schmucker et al., 2000).

1.4 Ack domain organization and function

Ack family genes generally contain a N-terminal SAM (sterile α- motif), tyrosine kinase, SH3 (Src homology 3), CRIB (Cdc42/Rac interacting/binding domain), proline-rich region, and C-terminal UBA domains (ubiquitin-associating domain; Figure 1A). Biochemical properties of these domains have been analyzed in vitro. The SAM domain facilitates the dimerization and membrane association of ACK1, and is essential for its function (Galisteo et al., 2006; Prieto-Echague et al., 2010). The function of the SH3 domain in ACK1 is less clear, although it has been proposed to auto-inhibit the kinase activity by forming an intramolecular complex with the proline-rich region (Lin et al., 2012). The UBA facilitates interaction with Nedd4 ubiquitin ligase and regulates ACK1 and substrate protein stability (Chan et al., 2009; Lin et al., 2010; Shen et al., 2007). The CRIB domain mediates interaction with Cdc42, although some Ack family genes lack a CRIB domain. Thus, while ACK1 was originally defined by its ability to bind GTP-bound Cdc42, distinct Ack members likely respond to Cdc42 activation differently. Additionally, despite the fact that dAck lacks the CRIB domain, it has a higher sequence similarity with ACK1 than PR2 especially in the activation loop raising the question of which is the true homologue of ACK1.

1.5 Ack binds to activated Cdc42, a key regulator for actin cytoskeleton

Tyrosine kinases are versatile signal transducers and contain regulatory domains capable of responding to specific stimuli (Blume-Jensen and Hunter, 2001). Among the non-receptor tyrosine kinase (NTK) families, ACK1 (activated Cdc42-associated kinase) is unique, as it contains a CRIB (Cdc42/Rac interacting and binding) domain and has the capability of directly interacting with the active form of the small GTPase Cdc42 (Manser et al., 1993). As Cdc42 is a critical regulator of actin cytoskeleton, cell migration, and cell polarity, this ability to bind to Cdc42 suggests ACK1 could mediate downstream effect of GTP-bound Cdc42. Consistent with this, ACK1 has been implicated in promoting metastasis (van der Horst et al., 2005), and its activity responds to ligand stimulation of integrin, a pathway known to facilitate cell migration (Eisenmann et al., 1999; Galisteo et al., 2006). However, the functional significance of this ACK1-Cdc42 interaction remains unclear.

1.6 Ack may play a role in clathrin dependent endocytosis

In *C. elegans* and cultured cells, Ack is known to negatively regulate EGFR signaling (Hopper et al., 2000; Shen et al., 2007), and one possible mechanism is that ACK1 facilitates clathrin-mediated internalization of EGFR (Grovdal et al., 2008). Indeed, ACK1 contains multiple clathrin-binding motifs and binds to clathrin and sorting nexin 9 in vitro (Shen et al., 2011; Teo et al., 2001; Worby et al., 2002; Yang et al., 2001; Yeow-Fong et al., 2005). In support of the notion that it has a role in clathrin-mediated endocytosis, overexpression of

ACK1 can stimulate receptor-mediated internalization of transferrin (Teo et al., 2001). In vivo, ACK1 is enriched in arrested clathrin-coated pits (Shen et al., 2011), although how it affects clathrin function remains unclear.

1.7 Ack in cancer

Deregulation of both mammalian Ack has been linked to cancers. ACK1 gene amplification or elevated ACK1 expression correlates with the ability of primary tumors to metastasize and poor prognosis in lung and prostate cancers (van der Horst et al., 2005). Somatic mutations in ACK1, some of which alter ACK1 activities, are detected in tumor samples (Prieto-Echague et al., 2010b). TNK1 appears to have a role in tumorigenesis as well, as high rate of spontaneous lymphomas and carcinomas were observed in TNK1 knockout mice (Hoare et al., 2008). ACK1 has been shown to phosphorylate and regulate the function of androgen receptor, WWOX, and AKT, highlighting the importance of tyrosine kinase activity (Mahajan et al., 2010; Mahajan et al., 2007; Mahajan et al., 2005). Tyrosine phosphorylation of ACK1 itself (e.g. tyr^{284} in the kinase domain), by either autophosphorylation or other tyrosine kinases, also influences its kinase activity (Yokoyama and Miller, 2003).Thus, a clearer understanding of the cellular function of Ack family genes should improve their potentials of being targets for anti-cancer treatments.

In this dissertation, chapters two and three will be dedicated to answering two main questions: What is the normal physiological function of Ack family in

Drosophila development and what is the physiological relevance of Ack family's ability to bind to activated Cdc42?

In chapter three we will describe the physiological role of Ack in Drosophila development mainly in spermatogenesis. We will show evidence of the autonomous requirement of Ack in germ cells for proper sperm formation. In addition, we will show that SAM, kinase, and SH3 domains are all essential for normal Ack function. Finally, we will describe how Dock localization is dependent on Ack kinase activity and on Dock's SH2 domain.

In Chapter four we will establish an over expression system of various Cdc42 constructs in testis. Expressing dominant active Cdc42, but not wild type or dominant negative Cdc42, causes cytokinesis defect in germ cells. We show that activated Cd42 localizes to the site of contractile ring constriction and disrupts anillin localization. The cytokinesis defect described is reduced by the loss of one copy of PR2 but not Ack. Additionally, this reduction is dependent on the CRIB domain but not the kinase activity. Moreover, PR2 is co-immunoprecipitated in complex with activated Cdc42 which also alters its cellular localization.

CHAPTER 2. MATERIALS AND METHODS

2.1 Fly genetics and molecular biology

All fly crosses were carried out at 25°C in standard laboratory conditions. To determine if the males of a particular genotype were sterile, three males of the genotype in question were mated with five w^{1118} virgins. If no eggs hatched after seven days, the genotype was considered sterile. *dj-GFP* flies were obtained from the Bloomington Stock Center (Bloomington, IN).

To construct pβ2tub-mCherry-Ack^{FL} and pβ2tub- GFP-PR2^{FL} plasmids, coding regions without stop codons of mCherry and GFP were PCR amplified and cloned into pβ2tub (Huh et al., 2004) and pUAST as EcoRI-NotI fragments, generating pβ2tub-mCherry(RN), pβ2tub-GFP(RN), pUAST-mCherry(RN), and pUAST-GFP(RN), respectively. Ack and PR2 coding sequences were excised from GH10777 and LD28966 (*Drosophila* Genomic Resource Center, IN), and fused in-frame with pβ2tub-mCherry(RN), pβ2tub-GFP(RN), pUAST-mCherry(RN), or pUAST-GFP(RN). The pβ2tub-mCherry-Ack deletions, pβ2tub-mCherry-Ack^{K156A}, and pβ2tub-mCherry-Ack^{CBM} mutants were generated by QuikChange kit (Agilent Technologies) and standard molecular biology techniques. Ack$^{\Delta S}$, Ack$^{\Delta U}$, and Ack$^{\Delta SH3}$ remove amino acids 1-90, 1013-1073, and 383-439, respectively. To construct pβ2tub-GFP-Rab and pβ2tub-GFP-dock

plasmids, Rab5^{wt}, Rab7^{wt}, Rab11^{wt} (Zhang et al., 2007), dock^{wt}, dock^{R336Q}, and dock^{3WK} (Rao and Zipursky, 1998) were PCR amplified and cloned into pβ2tub-GFP(RN) as NotI-XbaI fragments.

To generate pDJ-mCherry-Ack^{FL}, we first generated pDJ1 by replacing the *β2tub* promoter in pβ2tub with a 412 bps XhoI-EcoRI fragment (amplified by PCR), which contains *dj* upstream regulatory sequence and the 5'UTR (-320 to +83) (Blumer et al., 2002). mCherry-Ack^{FL} was excised from pβ2tub-mCherry-Ack^{FL} and cloned into pDJ1.

To generate pβ2tub-ACK1 and pβ2tub-TNK1 plasmids, ACK1 and TNK1 cDNAs were excised from pYX-Asc-ACK1 (clone 6400209; Openbiosystems) and pCMV-SPORT6-TNK1 (clone 4039780; Openbiosystems) and cloned into pβ2tub as EcoRI-NotI fragments. The TNK1 clone contained a missense mutation, changing the conserved Ala^{206} to a Thr, and was repaired by QuikChange.

All the above mentioned constructs were verified by sequencing (Purdue Genomics Core Facility), and transgenic flies were generated by P-element mediated transformation (Rubin and Spradling, 1982).

2.2 Antibody and immunofluorescence microscopy

Peptide corresponding to amino acid 494-505 (PHAKERKSTSSK) of Ack was used to generate rabbit polyclonal antibodies (Pacific immunology). Immunostaining of testes was performed according to Hime et al. (1996). Primary antibodies against Ack, PY (4G10; Millipore), Boss, and Lva (Sisson et

al., 2000) were used at 1:100, 1:100, 1:3000, and 1:100 dilutions, respectively. AlexaFluor-conjugated secondary antibodies, AlexaFluor-conjugated phalloidin (0.2U/µl, Molecular Probes), and Hoechst (12.3µg/µl, Thermo Scientific) were used at 1:200, 1:1000 and 1:10000, respectively. Fluorescence micrographs for rescue experiments and Boss staining were acquired at 25°C with 4× (0.13) and 60× (1.25) lenses on a Disk Scanning Unit-enabled Olympus BX61 microscope equipped with a Hamamatsu DCAM-API camera. All other micrographs were acquired with Zeiss LSM 710 laser scanning confocal microscope.

2.3 Quantification of elongated germ cell cysts

To count the cysts, testes from young (one day old) males, stained with Hoechst and phalloidin, were imaged on an Olympus BX-61 with Disk Spinning Confocal unit. Multiple 3D stacks (with 1µm stepping size), representing the entire testes, were acquired with a 40× (1.00) objective. The germ cell cysts in these stacks were then classified (based on the nuclear and IC morphology) and counted. The level of significance was determined by a Student's *t*-test. All quantitative data presented are the mean ± s.d from at least 14 testes.

2.4 Quantitative RT-PCR

Total RNA was isolated from dissected testes using RNeasy Mini Kit (Qiagen), and reverse transcribed into cDNA using iScript cDNA Synthesis Kit (Bio-Rad). For each PCR reaction, cDNA of approximately 1/8 of a testis was used as template. Reactions were performed on a 7300 Real-Time PCR System

(Applied Biosystems) and analyzed with 7300 System Sequence Detection Software (Applied Biosystems). The amount of *Ack* transcripts in each sample was normalized against the amount of actin (*Act5C*) transcripts from the same sample.

2.5 Co-immunoprecipitation and western analysis

Endogenous Dock immunoprecipitation experiments were preformed from testes extracts prepared from w^{1118} or $\beta 2tub\text{-}mCherry\text{-}Ack^{FL}$ adults. Immunoprecipitation of the mCherry-tagged Ack transgene was performed with lysates from $\beta 2tub\text{-}mCherry\text{-}Ack^{FL}$ adult testis co-expressing GFP-tagged $Dock^{wt}$, $Dock^{R3336}$, or $Dock^{3WK}$. Approximately 150 one-day old testes of appropriate genotypes were dissected in PBS, snap frozen in liquid nitrogen, and homogenized in 100µl of RIPA buffer (150mM NaCl, 1% Igepal CA-630, 0.5% sodium deoxycholate, 0.1% SDS, 50mM Tris pH 8.0, 0.2mM sodium orthovanadate, 10mM NaF, 0.4mM EDTA, 10% glycerol) at 4°C with a motorized pestle. Lysate volumes were adjusted to 400µl with RIPA buffer then sonicated with two 5 sec bursts of a microtip probe sonicator separated by chilling on ice. The lysates were cleared by sequential centrifugations of 15 min at 16,000xg and 30 min at 100,000xg. For endogenous Dock precipitation, 3µl of α-Dock antiserum was added and incubated for 1 hour on ice to form immune complexes, which were subsequently isolated by incubation with 30µl Protein-A agarose for one hour at 4°C with gentle rocking. For mCherry-Ack precipitation, 30µl RFP trap-A (ChromoTek) beads were added to lysates for one hour at 4°C with gentle

rocking. Beads containing immune complexes were washed with RIPA buffer three times and bound proteins were eluted in 30µl 2x SDS loading buffer at 95°C for 5 min. Samples were separated on 7.5% polyacrylamide gels, transferred onto Immobilon (Millipore) membrane using semi-dry transfer (BioRad; at 15V for 30 min), and probed with UM133 α-Dock (Clemens et al., 1996) or α-JCD2 antibody (Clemens et al., 2000) used at 1:1000 dilution. HRP-conjugated α-rabbit secondary (Rockland Immunochemicals) antibody was used at 1:10,000, and the blots were developed using Luminol Chemiluminescent HRP Substrate (Thermo Scientific).

Immunoprecipitation of Cdc42 was performed with lysates from β2tub-GFP-Cdc42^{wt} or β2tub-GFP-Cdc42^{G12V} co-expressing mCherry tagged PRFL or Ack^{FL}. Similar procedure was used as described above with minor adjustments: 30µl GFP trap-A (ChromoTek) used instead of RFP trap, αdsRed (Clontech) or αGFP were used at 1:1000 dilution to probe the membrane.

For western analysis of *β2tub-mCherry-Ack* constructs, 50 pairs testes of each genotype were dissected in PBS and homogenized in SDS loading buffer. Samples were boiled for 5 min, cleared by centrifugation at 16,000xg for 10 min, separated on 6% polyacrylamide gels, and transferred onto nitrocellulose membrane (Biorad). α-DsRed (Clontech) and HRP-conjugated α-rabbit secondary antibodies were used at 1:1000 and 1:10,000 dilutions in PBS, 0.1% Tween-20, respectively.

For western band intensity quantitation, films were scanned in Photoshop (Adobe) using a flatbed scanner (Canon 9950F) in transparency mode. Western

lane images were then analyzed using the Gel Analysis tools in ImageJ (National Institutes of Health) and the area under the peaks were measured. As α-Dock antibody detects a ~75kD background band in the control, the area of this background immunoreactive peak was subtracted from all experimental input areas. The IP peak area to adjusted input peak area ratios were calculated and normalized to GFP-dock^{wt}.

2.6 Cytokinesis defect quantification

To prepare squashed testis slides, young Adult males (1-2 days old) testis were dissected in TB (testis buffer) and single testis were transferred to a small drop of TB (less than 10µl) on 22x22mm coverslip. Using a fine tungsten wire, a nick was generated in the apical tip of the testis. While holding the basal end of the testis most of its contents are gently squeezed out using the tungsten wire. Afterwards, a glass slide is carefully brought close to the cover slip allowing them to attach together due to water adhesive forces (releasing the slide on the coverslip may lead to over squashed samples). The sample is then examined under a phase microscope for cells at the onion cell stage (64 cell stage). Images were quickly captured at 100X to be counted later. Each dark round circle is represents one mitochondria while each white circle corresponds to 1 nucleus. .

CHAPTER 3. ACK RECRUITS DOCK TO PROMOTE *DROSOPHILA* SPERMATOGENESIS

3.1 Loss of Ack disrupts sperm formation in *Drosophila* males

We have used *Drosophila* to investigate the function of Ack family genes during animal development. *Drosophila*, like mammals, has two Ack homologs, *Ack* (CG14992) and *PR2* (CG3969), located on 3rd chromosome left arm (64A6) and 2nd chromosome right arm (49F3), respectively. Although *Ack* is more similar to mammalian ACK1 in sequence, Ack lacks a CRIB domain, raising the question whether Ack is a true ortholog of ACK1. Complete removal of *Ack* function has been shown to disrupt dorsal closure during embryogenesis (Sem et al., 2002), but the penetrance of this phenotype is low. Instead, we show here that disruption of *Ack* function causes a fully penetrant absence of mature sperm, suggesting that spermatogenesis is a useful system for analyzing Ack function.

3.2 Drosophila spermatogeneis

Drosophila spermatogenesis consists of multiple well-defined and easily recognizable stages, which, in combination with mutational analysis, can be used to pinpoint gene functions. The spermatogonium, produced at the apical tip of testis by asymmetric germline stem cell division, undergoes additional cell divisions with incomplete cytokinesis to generate 64 haploid spermatids, (Gonczy

and DiNardo, 1996; Hardy et al., 1979). These round spermatids then elongate in a syncytium, reaching 1.8 mm in length (Lindsley and Tokuyasu, 1980). The elongated spermatids, interconnected through cytoplasmic bridges, are then separated through "individualization", a process characterized by coordinated movement of actin-based investment cones (ICs) along the axonemes (Tokuyasu et al., 1972). After individualization, bundles of mature sperm retract into basal coils and are deposited into the seminal vesicles.

3.3 Disruption of *Ack* function prevents the formation of mature sperms.

The loss-of-function mutation Ack^{86}, derived from imprecise excision of the P element line KG00869, contains a 2.7kb deletion extending to the beginning of the second exon of the *Ack* transcription unit (54 bps after ATG start; Fig. 1A) (Zahedi et al., 2008). To ensure that no Ack mRNA is generated by cryptic transcription initiation site, we performed quantitative RT-PCR analysis on testes mRNA using fluorogenic TaqMan oligonucleotides targeted against *Ack* exon2/3 junction (yellow box, Fig. 1A). While *Ack* mRNA was detected in w^{1118} and augmented in β*2tub-Ack*^{FL} (which expresses full-length *Ack* under germ cell-specific promoter; see below), it was absent in Ack^{86} (Fig. 1B), demonstrating that Ack^{86} is a null.

Most of Ack^{86} homozygous flies eclose with no significant morphological defects. The fact that Ack^{86} homozygous animals could survive to adulthood indicates that *Ack* is not an essential gene and no other recessive lethal mutations are present on the Ack^{86} chromosome. Ack^{86} females are fertile, but

Ack^{86} adult males are completely sterile. To understand the cause of this sterility, *dj-GFP* (*don juan*), which decorates the elongated mitochondria, was used to visualize spermatids in the testes and mature sperm in the seminal vesicles (Santel et al., 1998; Santel et al., 1997). Both *w*^{1118} (control) and *Ack*^{86} mutant testes contained *dj-GFP*-positive spermatids (arrows, Fig. 1C and D). However, while *dj-GFP*-positive sperm were seen in *w*^{1118} seminal vesicles (arrowhead, Fig. 1C), *Ack*^{86} seminal vesicles were empty (arrowhead, Fig. 1D), indicating that *Ack* has a role in sperm production.

3.4 *Ack*^{86} spermatids fail to coil properly.

The maintenance of germ stem cells and germ cell cytokinesis appeared normal in *Ack*^{86} testes (not shown), suggesting that removal of *Ack* function disrupts a late step of spermatogenesis. To further understand how loss of *Ack* function perturbs spermatogenesis, we stained one-day old *w*^{1118} and *Ack*^{86} testes with Hoechst and phalloidin to visualize germ cell cysts at various stages. In the coiled region, nuclear bundles before IC assembly, with IC assembling, and with IC departed were observed in both *w*^{1118} and *Ack*^{86} testes (Fig. 1E and H), suggesting that *Ack*^{86} does not affect IC assembly and migration. Consistent with this, the morphology of nuclear bundles and ICs, (Fig. 1F and I, insets) and the number of ICs at various stages (assembling, migrating, and disassembling; Fig. 1L) were comparable. However, while coiled spermatids were easily seen in control testes (Fig. 1C, a high magnification view in 1G), properly coiled

spermatids were not detected in *Ack*^{86} testes (Fig. 1D, a high magnification view in 1J).

To test whether *Ack*^{86} affects the progression of spermatid differentiation, elongated spermatids at various stages were counted. On average, *w*^{1118} testis (n=15) contained 63.0±13.0 elongated cysts, which were further assigned into categories of 34.1±8.7 (54.1% of elongated cysts) pre-IC assembly cysts, 17.3±4.8 (27.4%) cysts with assembling ICs, and 11.6±4.2 (18.5%) cysts with IC departed (Fig. 1K). In comparison, *Ack*^{86} testis (n=14) contained 64.1±11.2 elongated cysts, which consisted of 21.0±4.1 (33.0%) pre-IC assembly cysts, 19.1±4.4 (30.2%) cysts with assembling ICs, and 23.7±5.6 (36.8%) cysts with IC departed. Thus, while the numbers of total elongated germ cell cysts and those with assembling ICs were similar ($p=0.28$), *Ack*^{86} had less pre-IC elongated cysts ($p<0.001$), but more elongated cysts with IC departed ($p<0.001$). These observations suggest that in *Ack*^{86} testes, spermatids proceed to individualization early but fail to coil properly, resulting in an accumulation of elongated cysts with IC departed.

3.5 Ack is required cell autonomously for spermatogenesis.

To pinpoint the spatial and temporal requirement of *Ack* function for male fertility, we generated *β2tub-Ack*^{FL} and *β2tub-mCherry-Ack*^{FL}, which provide germ cell-specific expression of full-length untagged and mCherry-tagged Ack, respectively. As *β2-tubulin* promoter is only active in male germ cells at the primary spermatocyte stage (Kemphues et al., 1982), rescue of *Ack*^{86} sterility by *β2tub-*

Ack^{FL} would indicate that Ack function is required cell autonomously for spermatogenesis. In *β2tub-mCherry-Ack*^{FL} testes, mCherry-Ack^{FL} expression began at the spermatocyte stage, persisted throughout spermatid elongation, and decreased sharply after ICs began to migrate (Fig. 2A-C), confirming the specificity of *β2tub* promoter. Both *β2tub-Ack*^{FL} and *β2tub-mCherry-Ack*^{FL} rescued, as *β2tub-Ack*^{FL}*/+; Ack*^{86} and *β2tub-mCherry-Ack*^{FL}*/+; Ack*^{86} males contained dj-GFP-positive sperm in seminal vesicles and produced progeny when mated with *w*^{1118} females (compare Fig. 2H to 2G). The fact that *β2tub-mCherry-Ack*^{FL} rescued *Ack*^{86} demonstrates that mCherry-Ack^{FL} is functional. More importantly, these results indicate that Ack function for sperm production is required cell autonomously in the germ cells.

To further define when Ack is required, we placed *mCherry-Ack*^{FL} under *dj* control (*dj-mCherry-Ack*^{FL}), which contains translational regulatory elements to express transgenes post-meiotically (Blumer et al., 2002; Santel et al., 1997). Indeed, in *dj-mCherry-Ack*^{FL} testes, mCherry-Ack^{FL} expression was not detected in spermatids until IC assembly, but decreased sharply as ICs begin to migrate (Fig. 2D-F). Unlike *β2tub-mCherry-Ack*^{FL}, *dj-mCherry-Ack*^{FL} could not rescue *Ack*^{86} (Fig. 2I), indicating that Ack function is required at or after the spermatocyte stage but before IC assembly.

3.6 Mouse ACK1 can functionally substitute for Ack.

To determine whether mammalian ACK1 is a functional ortholog of Ack, transgenic flies expressing murine ACK1 and TNK1 under *β2tub* control (*β2tub-ACK1* and *β2tub-TNK1*, respectively) were generated. *β2tub-ACK1* restored fertility and sperm formation in Ack^{86} males (Fig. 2J). In contrast, germ cell-specific expression of TNK1, which lacks CRIB (similar to Ack), failed to rescue Ack^{86} sterility (Fig. 2J). These results demonstrate that ACK1, not TNK1, is the functional homolog of Ack.

To determine whether PR2, the other *Drosophila* Ack-related gene, could functionally substitute for Ack in sperm formation, we generated *β2tub-GFP-*$PR2^{FL}$ and tested its ability to rescue Ack^{86}. This GFP-$PR2^{FL}$ fusion is functional, as ubiquitous expression using UAS-GAL4 system (Act5C>*GFP-*$PR2^{FL}$) rescued the lethality of $PR2^{c02472}$ (a loss-of-function P element mutation of *PR2*). In differentiating male germ cells, mCherry-Ack^{FL} and GFP-$PR2^{FL}$ both appeared as vesicular structures around the cell periphery and showed considerable overlaps (Fig. 8). Nevertheless, *β2tub-GFP-*$PR2^{FL}$ could not rescue the sterility of Ack^{86}, indicating that Ack and PR2 are not functionally interchangeable for spermatogenesis (Fig. 2J).

3.7 The SAM, SH3, and kinase domains are indispensable for Ack function in male fertility.

To determine which Ack domains are critical for its function in spermatogenesis, we placed various Ack constructs under *β2tub* control (Fig. 3A),

and tested their ability to rescue *Ack*^{86} male sterility. These constructs include deletions removing the N-terminal SAM motif (Ack$^{\Delta S}$), the SH3 domain (Ack$^{\Delta SH3}$), and the C-terminal UBA (Ack$^{\Delta U}$). In addition, K156A and ^{549}LID→AAA substitutions have been introduced to disrupt the kinase domain (Ack^{K156A}) and a putative clathrin-binding box (Ack^{CB}), respectively. The abovementioned constructs were tagged with mCherry at the N-termini, and their expressions were verified by western analysis (Fig. 3B).

Similar to Ack^{FL}, germ cell-specific expression of Ack^{CB} and Ack$^{\Delta U}$ restored fertility and sperm production in *Ack*^{86} (Fig. 3E and F). In contrast, *β2tub-mCherry-Ack*$^{\Delta S}$, *β2tub-mCherry-Ack*^{K156A}, and *β2tub-mCherry-Ack*$^{\Delta SH3}$ failed to rescue *Ack*^{86} sterility (Fig. 3C, D, and G), indicating that the SAM domain, kinase activity, and the SH3 domain are critical for Ack function in sperm formation.

3.8 Ack associaes with peripheral clathrin positive structures

To understand how *Ack* contributes to sperm development at the cellular level, we determined its subcellular localization using both *β2tub-mCherry-Ack*^{FL} and rabbit polyclonal αAck antibody (Pacific Immunology, CA). Immunostaining of wild-type spermatocytes showed that Ack proteins are localized as vesicular structures around the cell periphery (Fig 9 A-C). This pattern was absent in *Ack*^{86}, demonstrating that our antibody is specific. Consistent with this, *β2tub-mCherry-Ack*^{FL}, which could restore fertility of *Ack*^{86}, exhibited a similar pattern.

To reveal the identity of these vesicular structures, we crossed *β2tub-mCherry-Ack*^{FL} with flies expressing fluorescently tagged organelle markers, including *β2tub-GFP-Clc* (clathrin; Fig. 4A-D), *β2tub-GFP-Rab5* (early endosome; Fig. 4E), *β2tub-GFP-Rab7* (late endosome/lysosome; Fig. 4F), *β2tub-GFP-Rab11* (recycling endosome; Fig. 4G), *β2tub-mito-GFP* (mitochondria; Fig. 4H), and *β2tub-myr-GFP* (plasma membrane; Fig. 4I). Of these, only GFP-Clc showed significant colocalization with mCherry-Ack^{FL}. *β2tub-GFP-Clc* labels peripheral (presumably endocytic) and internal clathrin-positive structures in spermatocytes (Zhou et al., 2011). The internal structures are secretory in nature, as they colocalized with Golgi/endosome-specific clathrin adaptor AP1 (Hirst et al., 2009; Zhou et al., 2011) and were in the vicinity of Lva- (lava lamp) positive structures (Fig. 4D). Although mCherry-Ack^{FL} colocalized extensively with peripheral clathrin-positive structures, it showed less overlap with secretory clathrin (Fig. 4A-D).

Consistent with the fact that Ack kinase activity is critical for its function in spermatogenesis, these peripheral Ack^{FL}-positive puncta were labeled by 4G10 anti-PY antibody (Fig. 9D); however, the level of 4G10 staining remained high around the cell periphery of *Ack*^{86} spermatocytes (Fig. 9E), indicating that Ack is not solely responsible for all the tyrosine phosphorylation events associated with these structures.

The fact that Ack associates with endocytic clathrin structures implies that Ack participates in clathrin-mediated endocytosis; however, Sevenless receptor-

mediated internalization of Boss (Bride of sevenless), a process known to depend on dynamin (Cagan et al., 1992; Kramer and Phistry, 1996), appeared unaffected in *Ack*^{86} eye discs (Fig. 4J-K). Comparable numbers of clusters containing internalized Boss (45.9% for wild type and 49.7% for *Ack*^{86}) were seen in both wild type and *Ack*^{86} eye discs. Furthermore, GFP-Clc distribution was unaffected in *Ack*^{86} spermatocytes, indicating that Ack has no role in regulating clathrin localization (Fig. 4L). Thus, although Ack co-localizes extensively with endocytic clathrin sites, we were unable to detect a role of Ack in clathrin-mediated endocytosis.

3.9 The SAM and SH3 domains are critical for Ack subcellular localization

To understand how Ack localizes to peripheral clathrin structures in spermatocytes, we analyzed the distribution of aforementioned Ack mutant proteins to define domains critical for its subcellular localization. As ACK1 is known to dimerize, the localization of these mCherry-tagged Ack mutants was analyzed in *Ack*^{86} background to avoid complication caused by dimerization with endogenous Ack. Consistent with the previous finding that the SAM domain is essential for ACK1 membrane association (Galisteo et al., 2006; Prieto-Echague et al., 2010a), the localization of mCherry-Ack$^{\Delta S}$ in differentiating germ cells appeared significantly disrupted (Compare Fig. 5B to 5A). In addition, the SH3 domain appears to have a role in Ack localization, as the pattern of mCherry-Ack$^{\Delta SH3}$ was predominantly cytoplasmic, not vesicular (Fig. 5F).

Similar to Ack^{FL}, Ack^{K156A} and $Ack^{\Delta U}$ exhibited significant spatial overlap with peripheral clathrin, indicating that kinase activity and the UBA domain are not essential for Ack localization (Fig. 5C and E). In addition, abolishing the putative clathrin-binding motif (Ack^{CB}) did not noticeably affect Ack colocalization with clathrin (Fig. 5D), suggesting that either this motif has no role in Ack protein distribution or an additional motif(s) contributes to Ack localization.

To ask whether Ack localization depends on clathrin, we first examined mCherry-Ack distribution in cells deficient in clathrin function. In *Chc*^{4} (a partial loss-of-function mutation in *clathrin heavy chain*) spermatocytes, mCherry-Ack localization appeared normal (Fig. 5G), implying that Ack subcellular localization is clathrin-independent. However, as this allele only partially disrupts clathrin (Peralta et al., 2009), the residual clathrin function in *Chc*^{4} might have been sufficient for localizing Ack (we were unsuccessful in generating mutant clones of spermatocytes using the strong *Chc*^{1} allele). Thus, to determine whether clathrin could recruit Ack, we took advantage of the fact that Ack in spermatocytes colocalizes mostly with endocytic sites and clathrin in salivary gland predominantly associates with secretory structures (Burgess et al., 2011). We reasoned that if the subcellular localization of Ack relies on clathrin, exogenously expressed Ack in salivary gland cells should associate with clathrin-positive structures in the secretory pathway. Indeed, mCherry-Ack exhibited significant spatial overlaps with secretory clathrin structures in *Act5C>mCherry-Ack* salivary gland cells (Fig. 5H-K), suggesting that clathrin is capable of influencing Ack localization.

3.10 Ack is required for Dock localization in male germ cells.

Mammalian ACK1 is known to bind to Nck, a SH2- and SH3-containing adaptor protein (Galisteo et al., 2006). Similarly, Dock, the *Drosophila* Nck homolog, interacts with Ack in S2 cells (Worby et al., 2002), although the significance of this interaction in vivo remains unclear. In flies, *dock* is an essential gene and has been implicated in axonal guidance and targeting (Desai et al., 1999; Garrity et al., 1996). To ask if Ack forms a complex with Dock during spermatogenesis, lysates prepared from w^{1118} and *β2tub-mCherry-Ack*^{FL} testes were immunoprecipitated with α-Dock antibody, followed by western analysis with α-Ack antibody (Fig. 6A). In w^{1118} extract, a faint band corresponding to the endogenous Ack was detected. Likewise, a band corresponding to the exogenously expressed mCherry-Ack was seen in *β2tub-mCherry-Ack* extract, indicating that Dock forms complex with Ack in testes. No Ack band was detected in the absence of α-Dock antibody (mock lanes), demonstrating the specificity of this interaction.

To determine the functional significance of this Ack-Dock interaction, we generated *β2tub-GFP-dock* (Fig. 6B) and asked if Dock localization in differentiating germ cells requires Ack. In early *β2tub-GFP-dock* primary spermatocytes, Dock appeared as puncta around the cell periphery (Fig. 6C) and at the ring canals (Fig. 10A-C). In late primary spermatocytes, Dock was localized to large vesicular structures (Fig. 10D). The presence of Dock in these structures persisted in secondary spermatocytes and pre-elongation spermatids, and detectable levels of Dock were seen in nuclei at these stages (Fig. 6D,

arrowheads). In elongating spermatids with canoe-shaped nuclei (not fully condensed), puncta intensely stained with Dock were seen in a region behind the nuclei at the nuclear ends (Fig. 6E, arrow) and in ring-like structures near the tail ends (Fig. 6F, arrowhead; inset). As spermatid elongation progressed, punctate Dock staining at the nuclear ends appeared to move farther away from the nuclei and became more compact (Fig. 6E, arrowhead). Similar to mCherry-Ack, Dock protein levels decreased prior to individualization (Fig. 6B).

During sperm differentiation, Dock colocalized extensively with Ack (Fig. 6G, arrowhead) and peripheral clathrin (Fig. 10), suggesting that Ack has a role in localizing Dock proteins. Indeed, vesicular Dock staining around the cell periphery was absent in Ack^{86} spermatocytes (Fig. 6H). In addition, the intense Dock staining beneath nuclei and the Dock-positive ring-like structures at tails ends of Ack^{86} elongating spermatids were also absent (not shown). Moreover, Dock subcellular distribution requires Ack kinase activity, as *β2tub-mCherry-*Ack^{FL}, but not *β2tub-mCherry-*Ack^{K156A}, restored vesicular Dock localization in Ack^{86} spermatocytes (Fig. 6I and J). It is worth mentioning that the presence of GFP-$dock^{wt}$ at the ring canals remained in Ack^{86} spermatocytes (Fig. 6H), indicating that not all of Dock localization depends on Ack.

3.11 Dock SH2 is essential for localization in male germ cells.

To ask which Dock domain is required for its localization, we generated *β2tub-GFP-*$dock^{3WK}$ and *β2tub-GFP-*$dock^{R336Q}$ (Fig. 7A), which provide germ cell-specific expression of mutant Dock with all three SH3 domains or the SH2

domain disrupted, respectively (Rao and Zipursky, 1998). Interestingly, while the level of GFP-dock^{wt} and GFP-dock^{R336Q} decreased before individualization, GFP-dock^{3WK} proteins persisted at high level after individualization (Fig. 7B and C), suggesting that SH3 domains have a role in regulating Dock protein stability. Nevertheless, in spermatocytes, GFP-dock^{3WK} appeared as puncta around the cell periphery, similar to those of wild type (Fig. 7D). In *β2tub-GFP-dock^{R336Q}* spermatocytes, Dock-positive vesicular structures were lost (Fig. 7E), demonstrating that the SH2 domain is critical for Dock subcellular localization. The dependence on the SH2 domain for Dock localization suggests that this domain contributes to Dock's ability to form a complex with Ack. To test this hypothesis, lysate from testes expressing mCherry-Ack^{FL} and various GFP-dock constructs (i.e. GFP-dock^{wt}, GFP-dock^{3WK}, and GFP-dock^{R336Q}) were immunoprecipitated with RFP-trap (ChromoTek), followed by western analysis with α-Dock antibody (Fig. 7F). While similar levels of GFP-dock^{wt} and GFP-dock^{R33Q} (indicated by the input lanes) were seen in lysates, less Dock^{R33Q} was detected in the precipitates (normalized intensity ratio (see M&M for details) of precipitated Dock^{R336Q}/input Dock^{R336Q} was 25.3% of precipitated Dock^{wt}/input Dock^{wt}), indicating that disruption of the SH2 domain strongly perturbs the formation of Ack-Dock complex. On the other hand, normalized intensity ratio of precipitated Dock^{3WK}/input Dock^{3WK} was 76.8% of precipitated Dock^{wt}/input Dock^{wt}, suggesting that SH3 domains have a lesser role in facilitating interaction with Ack.

CHAPTER 4. PR2 REDUCES ACTIVATED CDC42 CYTOKINESIS DEFECT

4.1 Expression of dominant active Cdc42 in male germ cells disrupts cytokinesis

Despite the fact that Cdc42 has been first identified by its ability to bind activated Cdc42 associated kinase, this binding remains poorly understood. Interestingly, only PR2 but not Ack has a CRIB domain raising the issue of importance of this domain for Ack function and suggesting that PR2 may be activated in a manner different than Ack. Indeed while Ack seems important for spermatogenesis, PR2 lethality reflects the necessity of PR2 function in normal growth and development. Additionally, neither the over-expression of PR2 in testis rescues Ack sterility, nor does Ack's ubiquitous expression rescues PR2 lethality further suggesting the two homologues exert different roles and may be under different control mechanisms. Since the two homologues have the same domain organization except for CRIB, we decided to further investigate the attributes of this domain. Mainly we are interested in understanding whether CRIB mediates interaction with Cdc42 and whether this interaction –if any- has physiological significance. To answer these questions we generated an over-expression system of wild type, dominant negative and dominant active Cdc42 in

testis. This system will be used to study the interactions between Cdc42 and Ack or PR2.

4.2 Expression of dominant active Cdc42 in male germ cells disrupts spermatogenesis

To ask whether deregulated Cdc42 activity affects *Drosophila* spermatogenesis, we expressed dominant active and negative Cdc42 mutants in differentiating male germ cells. Specifically, GFP-tagged $Cdc42^{wt}$, $Cdc42^{G12V}$, $Cdc42^{Q61L}$, and $Cdc42^{T17N}$ were placed under the control of *β2-tubulin* (*β2tub*) promoter (hereafter referred to as *β2tub-GFP-*$Cdc42^{wt}$, *β2tub-GFP-*$Cdc42^{T17N}$, *β2tub-GFP-*$Cdc42^{G12V}$, and *β2tub-GFP-*$Cdc42^{Q61L}$, respectively), which becomes active at the primary spermatocyte stage (Kemphues et al., 1982). *β2tub-GFP-*$Cdc42^{wt}$ males were fertile and seminal vesicles contained mature sperm (Figure 11A), indicating that overexpression of wild type Cdc42 in spermatocytes has no apparent adverse effect on fertility. Expression of dominant negative Cdc42 has no obvious impact on sperm formation, as *β2tub-GFP-*$Cdc42^{T17N}$ males were also fertile (Figure 11B). In contrast, *β2tub-GFP-*$Cdc42^{G12V}$ and *β2tub-GFP-*$Cdc42^{Q61L}$ males had reduced fertility, and their respective seminal vesicles contained few functional sperm (Figure 11C). To ensure that the GFP moiety did not affect male fertility, untagged $Cdc42^{wt}$, $Cdc42^{T17N}$, and $Cdc42^{G12V}$ were also placed under *β2tub* control. Similar to the tagged versions, the fertility of *β2tub*-$Cdc42^{wt}$ and *β2tub*-$Cdc42^{T17N}$ males appeared normal, whereas *β2tub*-$Cdc42^{G12V}$

males were sterile and had few sperm. There results indicate that ectopic activation of Cdc42 in differentiating male germ cells disrupts spermatogenesis.

4.3 Dominant active Cdc42 disrupts cytokinesis

To pinpoint the cause of male sterility, we monitored the progression of sperm development in these transgenic flies. While sperm differentiation in *β2tub-GFP-Cdc42^{wt}* and *β2tub-GFP-Cdc42^{T17N}* testes appeared normal, Hoechst and phalloidin staining showed that fully elongated *β2tub-GFP-Cdc42^{G12V}* and germ cell cysts contained scattered nuclei, abnormal IC assembly, and disorganized IC migration (compare Fig 11 B-C and F-G to J-K). However, in elongating *β2tub-GFP-Cdc42^{G12V}* spermatids, the defect of scattered nuclei was already seen (Figure 11K-number2), indicating that those phenotypes in fully elongated germ cell cysts were not the primary defects.

Examination of squashed testes under phase microscopy showed that ectopic Cdc42 activation in spermatocytes disrupts cytokinesis. In control testes, each spermatid contained one nucleus associated with one nebenkern (a mitochondrial derivative), indicative of normal male germ cell division (Figure 11G). In contrast, 42.3% of *β2tub-GFP-Cdc42^{G12V}* (n=482) and 25% of *β2tub-GFP-Cdc42^{Q61L}* (n=506) spermatids contained multiple nuclei associated with enlarged mitochondrial derivative (Figure 11L and data not shown). The extent of this cytokinesis defect is dose-sensitive, as flies carrying two copies of *β2tub-GFP-Cdc42^{G12V}* contained more multinucleated spermatids (62%; n=351) than those with only one copy. As the number, the size, and the morphology of *β2tub-*

GFP-Cdc42^{G12V} and *β2tub-GFP-Cdc42*^{Q61L} spermatocytes appeared normal, this cytokinesis defect represents the earliest phenotype associated with excessive Cdc42 activation (as the phenotypes of *β2tub-GFP-Cdc42*^{G12V} and *β2tub-GFP-Cdc42*^{Q61L} are similar, hereafter only *β2tub-GFP-Cdc42*^{G12V} results will be presented for the sake of clarity).

4.4 Expression of dominant active Rac and Rho1 in male germ cells does not affect cytokinesis

To ask whether constitutive activation of other Rho family members disrupts male germ cell cytokinesis, we generated *β2tub-Rho1*^{Q63L}, *β2tub-Rac1*^{Q61L}, and *β2tub-Rac2*^{Q61L}, which express activated Rho1, Rac1, and Rac2 under *β2tub* control respectively. *β2tub-Rac1*^{Q61L} and *β2tub-Rac2*^{Q61L} males had no discernible defect in fertility and germ cell cytokinesis (Fig 12A). In contrast, *β2tub-Rho1*^{Q63L} males exhibited reduced fertility and scattered ICs (compare Figure 12A to 12B). However, *β2tub-Rho1*^{Q63L} spermatids were not multinucleated, suggesting that deregulated Rho1 activation does not perturb spermatogenesis by disrupting germ cell cytokinesis (Figure 12). On the other hand, expression of a dominant negative Rho1 severely disrupts fertility and cytokinesis, as nearly all of the *β2tub-Rho1*^{T19N} spermatids (98.9%) contained 4 nuclei associated with nebenkern (Figure 12C; 4 is the maximal number of nuclei in this analysis because the transgenes become active at the primary spermatocyte stage). These results indicate that not all dominant interfering Rho

family mutants disrupt male germ cell divisions. Rather, the cytokinesis defects are specific to the expression of dominant negative Rho1 or constitutively active Cdc42.

4.5 Constitutively activate mutation alter the subcellular localization of Cdc42

To understand how $Cdc42^{G12V}$ disrupts germ cell divisions, we investigated the effect of the dominant active mutation on Cdc42 subcellular localization during cytokinesis. In *β2tub-GFP-Cdc42^{wt}* early and late primary spermatocytes, Cdc42 was predominantly cytoplasmic with elevated levels seen at the cell surface and the Golgi (Fig 13A-C). As the cells entered meiosis, Cdc42 became enriched at the sites of constriction and was present transiently at the contractile rings (Fig 14I-L and data not shown). After cytokinesis, $Cdc42^{wt}$ localization in spermatids resembled those seen in primary spermatocytes (i.e. along the plasma membrane and at the Golgi) (data not shown).

In *β2tub-GFP-Cdc42^{G12V}* early primary spermatocytes, the level of mutant Cdc42 in the cytoplasm and at the Golgi appeared diminished, whereas large aberrant $Cdc42^{G12V}$-containing structures were observed in the cytoplasm (Fig 13D). These $Cdc42^{G12V}$-positive structures were not Golgi, as they showed no association with either Lva or GM130 (Fig 13E-F, data not shown). At late spermatocyte stage, $Cdc42^{G12V}$ localized in aberrant structures at ring canals. (Fig 13J & Fig14E-H). During meiotic division, $Cdc42^{G12V}$ was seen at the sites of cell constriction in dividing cells as it co-localizes with anillin rings (Fig 14M-P).

4.6 Cdc42-positive aberrant structures contain elevated level of phosphotyrosine

The proximity of $Cdc42^{G12V}$ to the ring canal suggests that constitutive Cdc42 activation disrupts male germ cell divisions by perturbing the formation or maintenance of contractile rings. To test this, we examined the localization of ring canal components in *β2tub-Cdc42^{G12V}* male germ cells. The ring canals in fly male germ cells are known to contain PY, anillin, peanut, and septins (Neufeld and Rubin, 1994; Fares et al., 1995; Field and Alberts, 1995; Field et al., 1996; Hime et al., 1996). In *β2tub-GFP-Cdc42^{wt}* primary spermatocytes, anillin-RFP was seen in the nuclei and at the ring canals (Fig 14 A-D). As the cells divided, anillin-positive rings of various sizes, depending on the stage of cell divisions, were observed (Fig 14I-L). After meiosis, anillin rings were seen between cells and persisted in elongating spermatids (data not shown). In comparison, anillin staining in *β2tub-GFP-Cdc42^{G12V}* primary spermatocytes was disorganized, suggesting that activated Cdc42 associates with ring canal and disrupt its stability (Fig 14 E-H). Additionally, during cellular division, Cdc42 is enriched at the contractile ring also disrupting anillin staining.

To reveal the presence of PY-containing proteins, the germ cells were also stained with 4G10 antibodies. In *β2tub-Cdc42^{wt}* cells, PY appeared as puncta around cell periphery (Fig 13 G-I) with no significant overlap with $Cdc42^{wt}$. In *β2tub-Cdc42^{G12V}* spermatocytes, few punctate stained with PY were observed around cell periphery, but mostly PY was seen at the site of $Cdc42^{G12V}$ accumulation (Fig 13J-L). This change in PY localization due to Cdc42 activation

suggests that Cdc42^{G12V} potentially alters the localization of either PY kinases or their substrates from cell periphery to the contractile ring.

4.7 *PR2* suppresses Cdc42-dependent cytokinesis defects

The elevated PY staining in the aberrant Cdc42^{G12V}-positive structures (Fig 13 J-L) suggests that constitutively active Cdc42 disrupts cytokinesis by regulating tyrosine kinase(s) or phosphatase(s). As Ack family tyrosine kinases bind to GTP-bound Cdc42 directly (Manser et al., 1993), we asked whether *Ack* and *PR2*, the two *Drosophila* Ack homologs, are required for this Cdc42^{G12V}-dependent cytokinesis defect. Inactivating one copy of *Ack* (*Ack^{86}*/+) showed no significant effect on the phenotypic severity of *β2tub-Cdc42^{G12V}* (Fig 15A). In contrast, inactivating one copy of *PR2* by *PR2^{EM9}* (a EMS-induced allele-Fig 15A) or *PR2^{c02472}* (a PiggyBac insertion, data not shown) two independently isolated loss-of-function mutations, suppressed *β2tub-Cdc42^{G12V}*. These observations suggest that PR2, but not Ack, mediates the effect of Cdc42^{G12V} in disrupting male germ cell divisions.

To ask whether PR2 is the sole effector of Cdc42 in this context, we tested whether disrupting both copies of *PR2* would completely suppress Cdc42^{G12V}. To do this, we took advantage of the observation that neuron-specific expression of PR2 (*elav>PR2*) restored the viability of *PR2^{EM9}/PR2^{exi7}* mutants, thus producing adult males with germ cells deficient in PR2 function. Mutating both PR2 copies reduced the percentage of multinucleated *β2tub-Cdc42^{G12V}* spermatids from 52% to 1%, implying that PR2 is the major effector. Moreover,

these males are fertile suggesting that Cdc42 activation specifically disrupts cytokinesis but does not affect subsequent steps in division.

To determine which PR2 domain(s) is critical for mediating this $Cdc42^{G12V}$ effect, we took advantage of the fact that, complementary to the loss-of-function *PR2* alleles, PR2 overexpression in male germ cells (β*2tub-GFP-PR2*^{FL}) enhanced β*2tub-Cdc42*^{G12V} (Fig 15B). β*2tub-GFP-PR2*^{K164A}, which overexpresses a kinase-defective variant, enhanced β*2tub-Cdc42*^{G12V} to a similar extent (Fig 15B), suggesting that $Cdc42^{G12V}$ does not require PR2 tyrosine kinase activity to disrupt germ cell divisions. In contrast, the integrity of the SH3 domain is required for PR2 function in this context, as β*2tub-GFP-PR2*^{W438K} showed no significant interaction (Fig 15B). β*2tub-GFP-PR2*^{H497D}, which contains a defective CRIB domain, strongly suppressed β*2tub-Cdc42*^{G12V} (Fig 15B), suggesting that it is a dominant negative. Together, our results suggest that $Cdc42^{G12V}$ requires PR2 CRIB and SH3 domains to disrupt cytokinesis.

4.8 $Cdc42^{G12V}$ recruits PR2

To understand how Cdc42 activation influences PR2 function, we asked whether $Cdc42^{G12V}$ alters PR2 subcellular localization. Normally, PR2 is localized to internal puncta and vesicular structures around the cell periphery. These structures are distinct from those positive for Ack and clathrin (Fig 8). PR2 localization was studied in β*2tub-GFP-Cdc42*^{wt} and β*2tub-GFP-Cdc42*^{G12V} spermatocytes. As a control, the localization of mCherry-Ack in spermatocytes of

different genotypes was also determined. In *w*^{1118} and *β2tub-GFP-Cdc42*^{wt} control spermatocytes, vesicular PR2-positive structures were seen around the cell periphery and in internal regions, but showed few spatial overlap with tagged wild type Cdc42^{wt} (Fig 17G-I). Ack was also seen as vesicular structures around the cell periphery with few overlaps with Cdc42^{wt} (Fig 17A-C). In *β2tub-GFP-Cdc42*^{G12V} spermatocytes, Both PR2 and Ack were recruited to aberrant Cdc42^{G12V}-containing structures (Figs 17J-L & 17D-F respectively) suggesting that Ack and PR2 recruitment is CRIB independent or that they are recruited in different manners. At the time of writing this manuscript we were in the process of resolving this issue by testing the recruitment of various Ack and PR2 mutants by Cdc42.

To test whether PR2 forms a complex with Cdc42, extracts from testes expressing both *β2tub-mCherry-PR2*^{FL} and *β2tub-GFP-Cdc42*^{wt} or *β2tub-GFP-Cdc42*^{G12V} were subjected to co-IP analysis. While little mCherry-PR2 was precipitated with Cdc42^{wt}, the level of PR2 precipitated with Cdc42^{G12V} was significantly increased (Fig 17A). This suggests that PR2 binds to GTP-bound Cdc42.

As a control, in testis lysates expressing *β2tub-mCherry-Ack*^{FL} and *β2tub-GFP-Cdc42*^{wt} or *β2tub-GFP-Cdc42*^{G12V}, mCherry-Ack was not co-IPed with GFP-Cdc42^{wt} or GFP-Cdc42^{G12V} (Fig 17B). Additionally, to test whether Ack and PR2 are phosphorylated Ack and PR2 were IPed from w^{1118} testis lysates or testis expressing *β2tub-mCherry-Ack*^{FL}, *β2tub-mCherry-Ack*^{KD}, *β2tub-mCherry-PR2*^{FL},

or *β2tub-mCherry-PR2*^{FL}. Staining with 4G10 antibody, revealed that Ack has high tyrosine phosphorylation. On the other hand, the kinase defective mutant showed significantly less tyrosine phosphorylation, suggesting phosphorylation requires Ack kinase activity (auto or trans-phosphorylation). Additionally, PR2 was phosphorylated but to a lesser extent and this phosphorylation is kinase independent as the levels of PY didn't change between PR2^{wt} and PR^{KD}. The phosphorylation levels in all of these samples were not dependent on Cdc42 as the expression of the aforementioned constructs with Cdc42^{G12V} didn't alter their phosphorylation state significantly (data not shown).

CHAPTER 5. DISCUSSION

5.1 Ack is required for proper sperm formation

We show here that removal of Ack function completely disrupts sperm formation. Morphological examination suggests that the development of *Ack*^{86} germ cells progresses normally through cytokinesis, spermatid elongation, and individualization, but is disrupted at the coiling stage. Germ cell-specific expression of Ack restores fertility, indicating that the requirement of Ack function for spermatogenesis is cell autonomous. Using *dj-mCherry-Ack*, we further refine the temporal requirement of Ack function to a period between spermatocyte stage and IC assembly. Thus, although the developmental defects of *Ack*^{86} germ cell cysts are manifested at the coiling stage, the time of action for Ack in spermatogenesis is earlier.

Mammals and *Drosophila* both have two Ack-related genes, differing by the presence of CRIB domain. Although Ack resembles TNK1 in domain organization (both lack CRIB), it exhibits higher sequence similarity to ACK1. Rescue experiments show that ACK1, but not TNK1, can functionally substitute for Ack during spermatogenesis. These observations demonstrate that ACK1, while containing CRIB, is the functional homolog of Ack.

5.2 Ack and PR2 are not redundant

Given that Ack is widely expressed during development and interacts with two essential genes (*Cdc42* and *dock*), it is surprising that mutants homozygous for Ack^{86}, a null allele, could survive till adulthood. One possible explanation for this weak phenotype of Ack^{86} in animal viability is that Ack-mediated cellular processes are redundant for viability, but spermatogenesis is particularly sensitive to the absence of Ack because of its unusual morphogenesis. Indeed, this phenotypic specificity has been observed in mutants of several genes regulating Golgi function (e.g. *four way stop* (*fws)* and *Brunelleschi* (*bru*)), which are thought to provide lipids to fulfill the high membrane demand required for male germ cell divisions (Farkas et al., 2003; Robinett et al., 2009). Alternatively, it is possible that *PR2*, the other *Drosophila* Ack-related gene, could compensate in essential functions. However, unlike *Ack*, removal of *PR2* function causes animal lethality, indicating that Ack and PR2 have non-overlapping functions during development. The difference in Ack and PR2 subcellular localizations also suggests that they have distinct cellular roles. In support of this, germ cell-specific expression of PR2 fails to rescue Ack^{86}-associated sterility. Thus, although related in sequence and domain organization, Ack and PR2 are not functionally redundant, even when expressed in the same cells. Rescue experiments with chimeras are needed to define domains conferring specificities to these Ack family genes.

5.3 Ack doesn't impact the apoptotic machinery in spermatogenesis

During spermatid individualization, the apoptotic machinery is thought to facilitate the breakdown of cellular organelles in waste bags. In support of this, cleaved caspase-3 staining can be seen ahead of migrating ICs (Huh et al., 2004), and disruption of cell death genes causes defects in individualization and sperm formation (Arama et al., 2003; Huh et al., 2004). It has been recently demonstrated that Ack has anti-apoptotic function in response to EGF signaling during eye development, and the level of caspase-3 activation increases slightly in individualizing Ack^{86} germ cell cysts (Schoenherr et al., 2012). These observations suggest that Ack^{86} may abolish sperm formation by disrupting the function of cell death genes. However, *Ack*, while required for male fertility, does not appear to function during individualization, as IC assembly and migration were normal in Ack^{86} spermatids. Thus, while an anti-apoptotic role of Ack during eye development is evident (Schoenherr et al., 2012), whether Ack regulates apoptotic genes during spermatogenesis requires further investigation.

5.4 Ack associates with clathrin positive structures

In spermatocytes, functional mCherry-Ack associates mostly with clathrin-positive structures around the cell periphery, and less with those in the secretory pathway. This distribution of Ack proteins is not caused by overexpression, as endogenous Ack proteins, revealed by antibody staining, exhibit a similar distribution. Our results are consistent with the observation that mammalian ACK1 associates with clathrin-positive structures in cultured cells, especially in

those expressing GTP hydrolysis-defective dynamin (Shen et al., 2011). This association of Ack with peripheral clathrin sites suggests that it participates in clathrin-mediated endocytosis. Indeed, ACK1 has been shown to regulate the internalization of transferrin receptor and EGFR (Grovdal et al., 2008; Teo et al., 2001). *C. elegans* SID-3, an Ack-related protein, has recently been shown to mediate the intercellular transport of dsRNA (Jose et al., 2012). However, using a Boss internalization assay in eye discs, we were unable to detect endocytic defects in Ack^{86} animals. In addition, clathrin localization appears unperturbed in spermatocytes completely lacking Ack function. Thus, while a role of Ack in clathrin-mediated endocytosis cannot be excluded, our results suggest that this role, if there is one, is either minor or cargo-specific.

Clathrin-mediated transport has been suggested to facilitate lipid transport from the Golgi to sustain the membrane increase required for spermatid elongation (Zhou et al., 2011). The association of Ack with clathrin suggests that it could have a role in regulating this lipid transport required for the rapid membrane growth. However, in spermatocytes, Ack localizes preferentially to clathrin-positive structures around the cell periphery, which are endocytic in nature. More importantly, Ack^{86} phenotype in sperm development is distinct from those of *fws*, *bru*, and *Chc* (Fabrizio et al., 1998; Farkas et al., 2003; Robinett et al., 2009). In addition, the staining of myr-GFP (which labels the plasma membrane) in Ack^{86} elongated spermatids appeared normal (not shown). Collectively, these observations do not support a role of Ack in providing membrane for spermatid elongation.

How does Ack localize to endocytic clathrin sites? A putative clathrin-binding motif (549-LIDIS) has been reported for Ack (Teo et al., 2001), although we show that disruption of this motif has no apparent effect on Ack localization and function in spermatogenesis. In vitro analysis has shown that murine ACK1 interacts directly with clathrin via two motifs, 496-LLSVE and 584-LIDFG (Shen et al., 2011). However, $ACK1^{A4}$, which bears mutations inactivating both motifs, remains associated with clathrin-positive structures in cells, implying that interaction other than ACK1-clathrin binding contributes to ACK1 localization (Shen et al., 2011). It is possible that, like ACK1, Ack contains additional motifs capable of interacting with clathrin directly and is localized to endocytic sites by other interactions.

5.5 SAM and SH3 contribute to Ack proper localization

Analysis of the deletion constructs suggests that the SAM and SH3 domains are critical for Ack subcellular localization. Consistent with our observations, SAM has been demonstrated to mediate ACK1 dimerization and membrane association (Galisteo et al., 2006; Prieto-Echague et al., 2010a). The SH3 domain, while not known to contribute to ACK1 localization, has been shown to regulate ACK1 kinase activity (Lin et al., 2012). This raises a possibility, in which the SH3 deletion disrupts Ack localization by perturbing Ack kinase activity. However, the fact that Ack^{K156A} localizes properly argues against this scenario, as Ack kinase activity does not appear to have a role in Ack localization. It may be that SH3 facilitates the recruitment of Ack to endocytic clathrin

structures by binding to PPXP-containing signaling molecules already present in clathrin sites. It is critical to identify factors interacting with SAM and SH3 to pinpoint how these domains contribute to Ack function and subcellular localization. In any case, the fact that SAM and SH3 domains are also essential for Ack function in sperm production suggests that the localization of Ack to endocytic clathrin sites contributes to its function in sperm formation.

5.6 Proper Dock localization in germ cells is dependent on Ack

ACK1 is known to interact with Nck, an adaptor with three SH3 domains and a C-terminal SH2 domain (Galisteo et al., 2006; Teo et al., 2001). In *Drosophila*, *dock*, the Nck homolog, has been implicated in axonal targeting of photoreceptors (Garrity et al., 1996), but its role in male germ cell development has not been investigated. We show that Dock colocalizes with Ack extensively during spermatogenesis, and the presence of Dock puncta around the cell periphery in spermatocytes requires Ack. Immunoprecipitation experiments further show that Dock and Ack form a complex in testes. Together, these results suggest that Ack recruits Dock to endocytic sites to facilitate sperm formation.

The fact that *dock*, but not *Ack*, is an essential gene suggests *dock* has functions that are Ack-independent. Indeed, Dock localization near the ring canals remains in Ack^{86} spermatocytes, indicating that not all Dock localization is Ack-dependent. These ring canals, derived from incomplete cytokinesis of differentiating male germ cells, are known to contain PYs (Hime et al., 1996),

suggesting that SH2-PY interaction is important for localizing dock to the rings as well. In support of this, disruption of the SH2 domain renders Dock cytoplasmic in spermatocytes. Thus, while the identity of the putative tyrosine kinase(s) responsible for recruiting Dock to the ring canals remains unclear, our results suggest that Dock localization during spermatogenesis depends on at least two tyrosine kinases.

Rescue analysis indicates that Ack kinase activity is required for spermatogenesis. In cancers, phosphorylation by ACK1 has been suggested to activate AKT by facilitating recruitment of AKT to the membrane (Mahajan et al., 2007). Two lines of evidence suggest that Akt is not a relevant substrate for Ack under physiological conditions. First, *β2tub-Akt*^{myr}, which provides germ cell-specific expression of a membrane associated Akt (*Drosophila* Akt tagged with a myristylation signal), does not rescue *Ack*^{86} sterility (not shown). In addition, *Akt* does not interact genetically with *Ack* during eye development (Schoenherr et al., 2012). Instead, given that SH2 is critical for Dock localization, we propose that Ack-dependent tyrosine-phosphorylation provides PYs for recruiting Dock to specific sites during spermatogenesis. Indeed, while Ack^{FL} rescues male fertility and Dock localization, Ack^{K156A}, even though being localized properly, is unable to restore Dock subcellular distribution. The fact that Ack^{K156A} localizes properly in cells with mislocalized Dock suggests that Ack localization does not rely on Dock. Future experiments are needed to determine whether this Ack-dependent Dock localization is mediated by PYs in Ack generated by autophosphorylation or by Ack-dependent phosphorylation of another protein.

5.7 Ack recruits Dock and potentially WASp to promote *Drosophila* spermatogenesis

Nck is known to interact with WASp, an actin nucleation protein, via multivalent SH3/PPxP interactions (Rivero-Lezcano et al., 1995; Rohatgi et al., 2001). Interestingly, disruption of WASp and Cdc42 function in cyst cells has been shown to non-cell autonomously impair spermatid docking and maturation (Rotkopf et al., 2011). While a cell autonomous role of WASp in sperm formation has not been demonstrated, our analysis of *Ack* and *dock* certainly supports this possibility. Consistent with this, WASp in elongated spermatids colocalizes with Dock in the region underneath partially condensed nuclei and this WASp localization is Ack-dependent (A.A. manuscript in preparation). It is possible that recruitment of Dock and WASp by Ack near the nuclear ends of elongating germ cells also contributes to spermatid docking, and disruption of which renders spermatids incapable of coiling.

5.8 Over-expression of $Cdc42^{G12V}$ causes cytokinesis defects in germ cells

Expression of dominant active Cdc42 in Drosophila embryos causes cytokinesis defects. Similarly, we show that the expression of $Cdc42^{G12V}$ in germ cells under *β2Tub* promoter disrupts cytokinesis during meiotic division in spermatogenesis. This cytokinesis defect is specific to over-expressing the activated form of Cdc42 and not the wild type ($Cdc42^{wt}$) nor the dominant negative ($Cdc42^{T17N}$). This defect also leads to reduced fertility as less sperms are produced and deposited into the seminal vesicles. Additionally, the defect is

dose dependent as the expression of multiple copies of Cdc42 increase the cytokinesis defect.

5.9 $Cdc42^{G12V}$ is recruited to the contractile rings

On the cellular level we noticed that the localization of $Cdc42^{G12V}$ is very different from the $Cdc42^{wt}$. While $Cdc42^{wt}$ localizes around cell periphery and in Golgi positive puncta, $Cdc42^{G12V}$ was mostly localized to a large aberrant structure around cell periphery. When stained with PY, this structure was highly phosphorylated, suggesting that Cdc42 is recruiting tyrosine kinases/substrates into this location. To further understand the nature of this structure we used the contractile ring marker anillin. anillin, in addition to PY, peanut, and septins, is a part of the protein machinery required for ring formation and constriction. anillin localized extensively with $Cdc42^{G12V}$ but not with $Cdc42^{wt}$. Additionally, anillin formed intact contractile rings in $Cdc42^{wt}$, but these rings were disrupted in $Cdc42^{G12V}$ indicating that activated Cdc42 is present at the site of ring formation.

5.10 $Cdc42^{G12V}$ recruits PR2

When stained with PY marker, $Cdc42^{G12V}$ caused aberrant structure seems to be highly phosphorylated indicating one or more tyrosine kinases are being recruited to this site. We asked whether Ack and PR2 are recruited to the site of ring formation. Indeed, both Ack and PR2 are recruited to this site as seen by immunofluorescence. However, through IP experiments we showed that PR2 but not Ack is co-IPed in complex with activated Cdc42, suggesting that Ack is

recruited to the contractile ring indirectly. We are currently investigating the requirement of CRIB domain to bind to $CDC42^{G12V}$ through Co-IP of Cdc42 and various PR2 complexes. In addition, we are studying the localization of these various complexes wits Cdc42 using immunofluorescence.

5.11 Loss of PR2 reduces the cytokinesis defect

The cytokinesis defect generated by $Cdc42^{G12V}$ provided us with a quantitative assay to study genetical interactions with Cdc42. Indeed the removal of one copy of PR2 but not Ack reduces the cytokinesis defect significantly. Moreover, the over-expression of $PR2^{wt}$ causes significant increase in the cytokinesis defect, and this increase is dependent on the CRIB domain but not on PR2 kinase activity. In fact, an over-expression of a mutant CRIB domain decreases the cytokinesis defect and acts similar to a dominant negative. Another observation that is worth noting was that the over-expression of the SH3 mutant neither increased nor decreased the cytokinesis defect significantly indicating that SH3 domain is also important for PR2 function in this context.

Taken together, these data suggest that the CRIB domain is essential for the recruitment of PR2 to the site of contractile ring formation. We hypothesize that upon recruitment, PR2, in turn, can recruit other effectors that disrupt cytokinesis through its SH3 domain. It's appealing to speculate that anillin or maybe one or more of the other ring forming proteins may directly or indirectly interact with the PR2.

5.12 Ack and PR2 in disease

As ACK1 amplification has been linked to enabling metastasis, a better understanding of Ack cellular function can clearly benefit the battle against cancers. Our demonstration that Ack and Dock are essential for male sterility provides a robust process to further dissect the functions of these two genes. In addition, *Drosophila* spermatogenesis, with its accessibility to genetics and cell biological manipulations, should aid in identifying and characterizing upstream regulators and downstream effectors of this important pathway. Moreover, our work on the link between PR2 and Cdc42 shows that there is some physiological significance to the binding between activated Cdc42 and PR2. Since Cdc42 is a key cytoskeletal actin regulator, it would be interesting to see if this interaction contributes to cancer metastasis. If so, studying how deregulation of PR2 can alter the cytoskeletal reorganization in cells may prove very useful in designing future drugs and therapeutics.

Figure 1.**Ack is required for spermatogenesis.** (A) A schematic representation of *Ack* genomic region. The *Ack* coding sequence and untranslated regions are represented by filled and open boxes, respectively. The transposon KG00869 is inserted 4 bps 5' to the putative transcription start site. In Ack^{86}, a deletion allele generated from the excision of KG00869, the first exon, intron, and the ATG start sequences are removed (the extent of deletion is indicated by dashed arrow). The yellow box denotes the fluorogenic TaqMan oligonucleotides used in panel B. While lacking the CRIB domain, Ack contains SAM (orange), tyrosine kinase (purple), SH3 (green), and UBA (blue). (B) Quantitative RT-PCR analysis of *Ack* mRNA abundance in testis RNA of various genotypes. (C-J) Laser scanning confocal micrographs of dj-GFP-expressing w^{1118} (C, E-G) and Ack^{86}/Ack^{86} (hereafter referred as Ack^{86}; D, H-J) testes stained with phalloidin (red) and Hoechst (blue). In C and D, dj-GFP-positive spermatids (indicated by arrows) are seen in both w^{1118} and Ack^{86} testes. In contrast, dj-GFP-positive mature sperm are only seen in w^{1118} seminal vesicles (indicated by arrowheads). Scale bar = 100μm. In E and H, elongated germ cell cysts at the stage before IC assembly (denoted by 1), with IC assembling (denoted by 2), and with IC departed (denoted by 3) are seen in both w^{1118} and Ack^{86} testes. IC migration (F and I) and morphology (insets) in w^{1118} and Ack^{86} testes appear comparable. However, while spermatid coiling is readily observed in w^{1118} (G), this process is disrupted in Ack^{86} testes (J). Scale bar = 20μm. (K-L) Quantification of the number of elongated germ cell cysts (K) and ICs (L) at various stages in w^{1118} and Ack^{86} testes. For each category, the mean + standard deviation are shown (n=15 for w^{1118}, n=14 for Ack^{86}; * indicates $p<0.001$). The level of significance was determined by a Student's *t*-test.

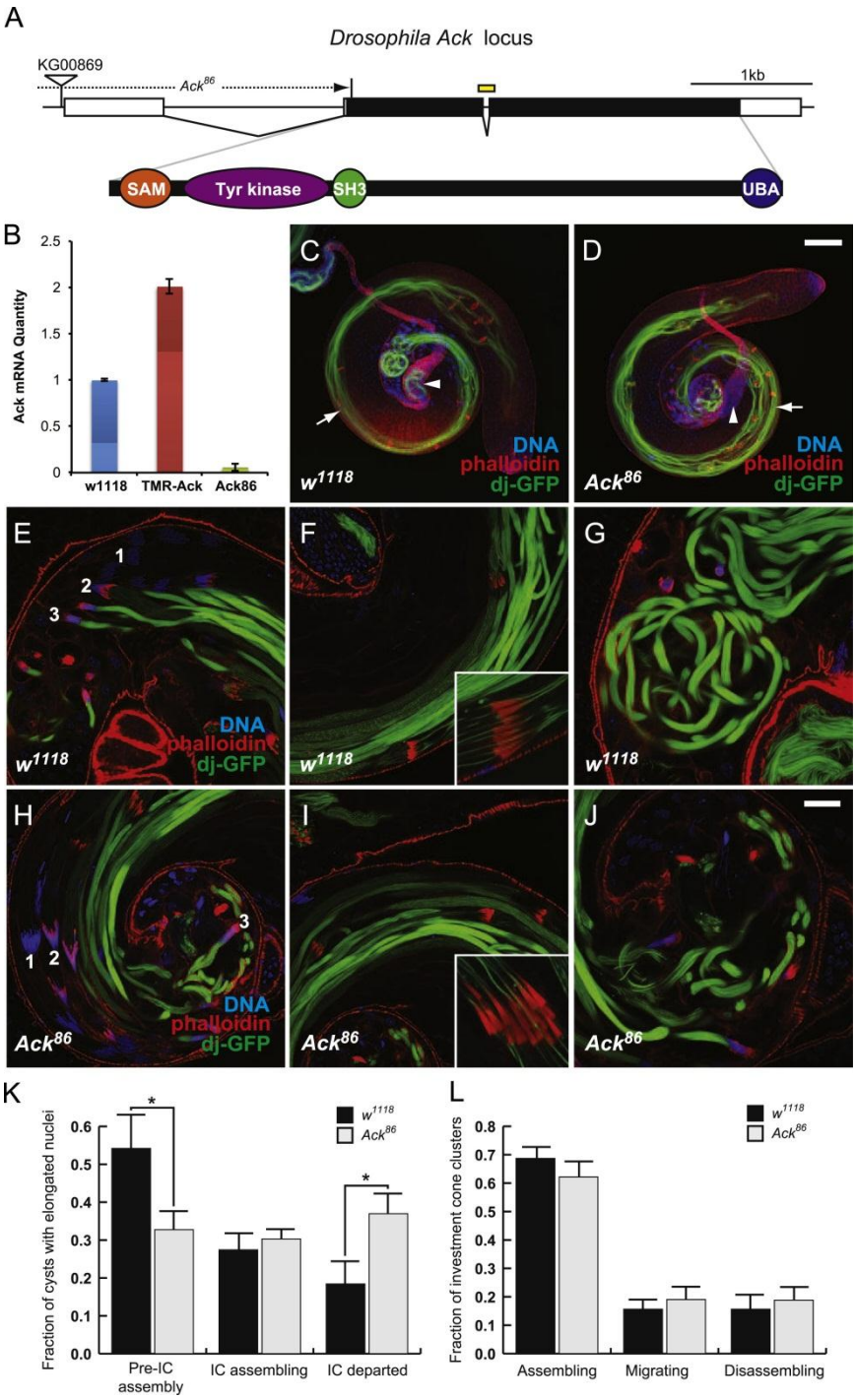
A
Drosophila Ack locus
KG00869
Ack86
1kb
SAM
Tyr kinase
SH3
UBA
B
Ack mRNA Quantity
w1118
TMR-Ack
Ack86
C
D
DNA
phalloidin
dj-GFP
w1118
Ack86
E
F
G
H
I
J
1
2
3
K
Fraction of cysts with elongated nuclei
Pre-IC assembly
IC assembling
IC departed
L
Fraction of investment cone clusters
Assembling
Migrating
Disassembling

Figure 1.

Figure 2.The requirement of Ack function in spermatogenesis is cell autonomous. (A-F) Fluorescent micrographs of *β2Tub-mCherry-Ack*^{FL} (A-C) and *dj-mCherry-Ack*^{FL} (D-F) testes stained with phallodin (green) and Hoechst (blue). Solid and dashed boxes in A and D are shown at higher magnification in B and E, and C and F, respectively. In *β2Tub-mCherry-Ack*^{FL}, expression of exogenous Ack is seen in spermatocytes (indicated by arrowheads and denoted by 1 in B), pre-IC assembly elongated spermatids (denoted by 2; inset in C), elongated spermatids with IC assembled (indicated by arrow and 3 in C). In contrast, expression of exogenous Ack in *dj-mCherry-Ack*^{FL} is not seen until elongated spermatids with IC assembled (indicated by arrow and 3 in F). In both *β2Tub-mCherry-Ack*^{FL} and *dj-mCherry-Ack*^{FL}, mCherry-Ack level decreases sharply when IC migration begins (indicated by arrowheads and 4 in C and F). (G-I) Spinning disc confocal micrographs of *Ack*^{86} (G), *Ack*^{86}*; β2Tub-mCherry-Ack*^{FL}/+ (H), and *Ack*^{86}*; dj-mCherry-Ack*^{FL}/+ (I) testes expressing dj-GFP. Seminal vesicles connected to the coiled regions of the testes are indicated by arrows. Scale bar = 100μm. (J) A schematic representation of *Drosophila* and mouse Ack family genes. ACK1 and PR2 contain SAM (orange), tyrosine kinase (purple), SH3 (green), CRIB (light blue), and UBA (dark blue). In contrast, TNK1 and Ack lack CRIB. The ability of these genes to rescue *Ack*^{86}-associated male sterility is shown on the right (+ for rescue and – for fail to rescue)

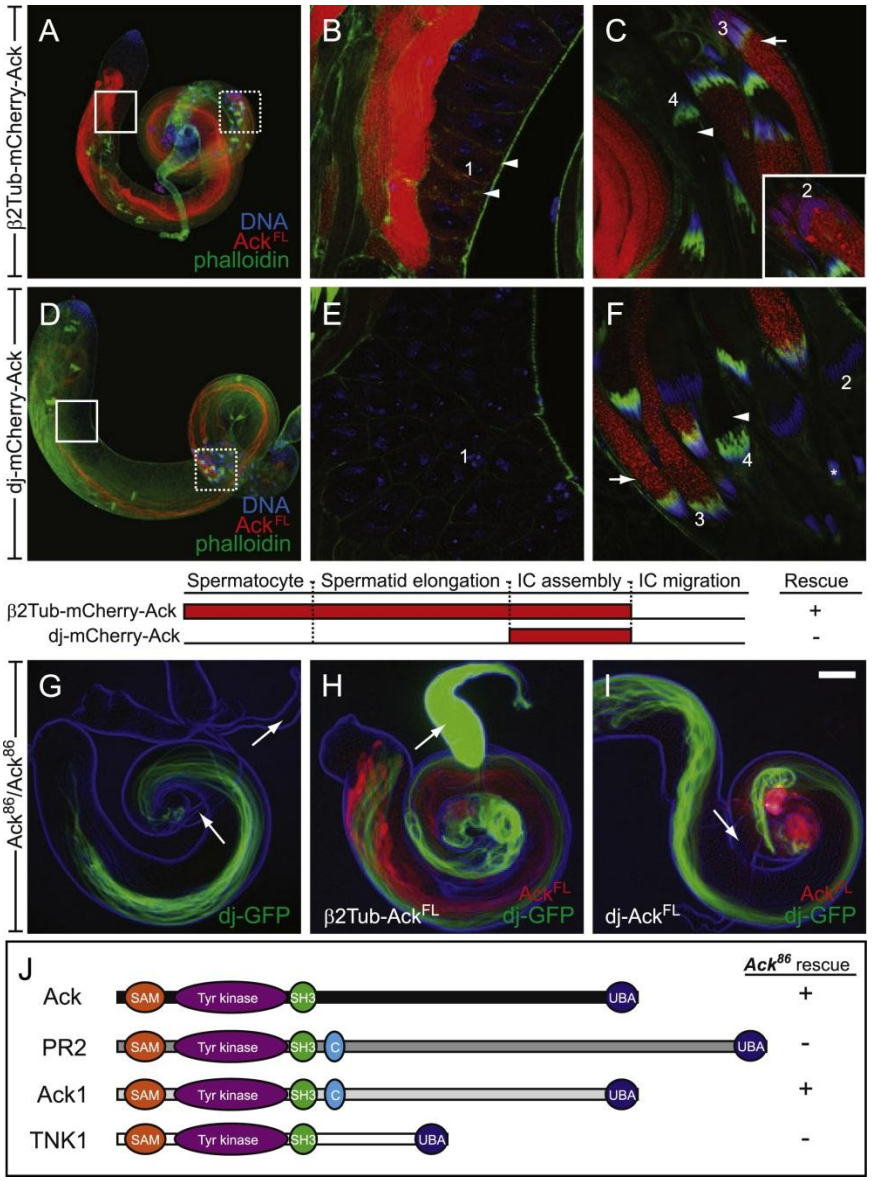
β2Tub-mCherry-Ack
dj-mCherry-Ack
Ack86/Ack86
A
B
C
D
E
F
G
H
I
J
DNA
AckFL
phalloidin
Spermatocyte
Spermatid elongation
IC assembly
IC migration
Rescue
β2Tub-mCherry-Ack
dj-mCherry-Ack
+
-
dj-GFP
β2Tub-AckFL
dj-AckFL
Ack86 rescue
Ack
PR2
Ack1
TNK1
SAM
Tyr kinase
SH3
C
UBA

.Figure 2.

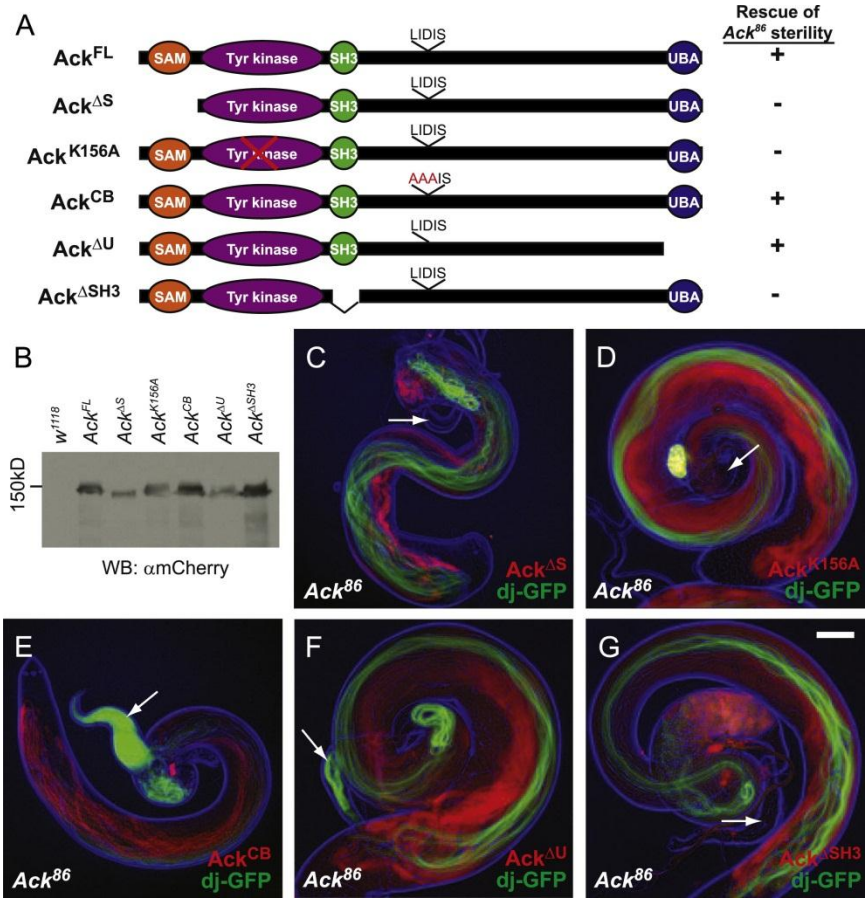

Figure 3. Ack function in spermatogenesis requires SAM, tyrosine kinase, and SH3. (A) A schematic representation of *Ack* deletion and point mutants. ΔS, ΔU, and ΔSH3 remove the SAM (orange), UBA (blue), and SH3 (green), respectively. K156A and CB are substitutions affecting the kinase (purple) and LIDIS motif. The ability of these exogenous expressed *Ack* constructs to rescue *Ack*^{86}-associated male sterility is indicated on the right. (B) Western analysis of *mCherry-Ack* testis extracts probed with α-DsRed antibody. While no band is seen in *w*^{1118} control, bands of expected sizes (mCherry-Ack^{FL}=145.3kD, mCherry-Ack$^{\Delta S}$=135.1kD, mCherry-Ack$^{\Delta U}$=138.9kD, and mCherry-Ack$^{\Delta SH3}$=139.0kD) are detected in *mCherry-Ack* lanes. (C-G) Spinning disc confocal micrographs of *Ack*^{86}; *dj-GFP* testes carrying *β2Tub-mCherry-Ack*$^{\Delta S}$/+ (C), *β2Tub-mCherry-Ack*^{K156A}/+ (D), *β2Tub-mCherry-Ack*^{CB}/+ (E), *β2Tub-mCherry-Ack*$^{\Delta U}$/+ (F), and *β2Tub-mCherry-Ack*$^{\Delta SH3}$/+ (G). Seminal vesicles are indicated by arrows. Scale bar = 100μm.

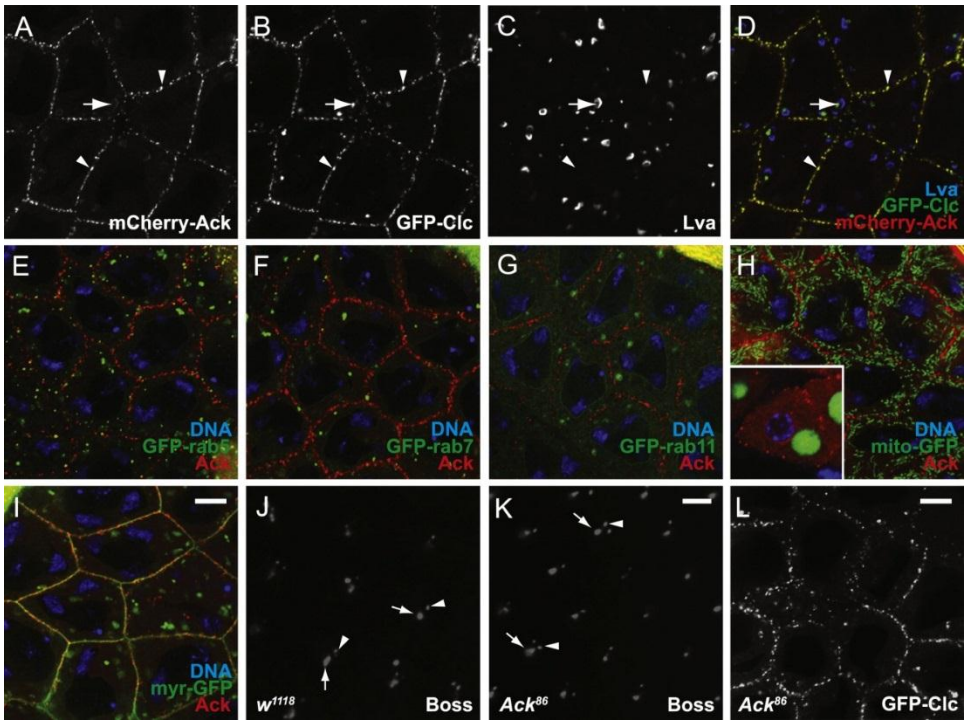

Figure 4. Ack is localized to endocytic clathrin structures in spermatocytes. (A-D) Laser scanning confocal micrographs of *β2Tub-mCherry-Ack*^{FL}**,** *β2Tub-GFP-Clc* spermatocytes stained with α-Lva antibody (blue in D). Ack (A) exhibits overlaps with clathrin (B) around the cell periphery (arrowheads), but less with those that are near Lva-positive structures (C, arrow). (E-I) Confocal micrographs of *β2Tub-mCherry-Ack*^{FL} spermatocytes carrying *β2Tub-GFP-rab5* (E)**,** *β2Tub-GFP-rab7* (F)**,** *β2Tub-GFP-rab11* (G)**,** *β2Tub-mito-GFP* (H), and *β2Tub-src-GFP* (I). Inset in (H) shows spermatids expressing mCherry-Ack^{FL} and mito-GFP. DNA is shown in blue. Scale bar = 5μm. (J-K) Fluorescent micrographs of *w*^{1118} (J) and *Ack*^{86} (K) eye discs stained with α-Boss antibody. Boss, a transmembrane ligand expressed on the apical surface of R8 cells (big dots indicated by arrows), is internalized into neighboring cells (trailing smaller dots indicated by arrowheads) via clathrin-mediated endocytosis. Comparable level of Boss internalization is seen in both *w*^{1118} and *Ack*^{86} eye disc cells. Scale bar = 5μm. (L) Confocal micrograph of *Ack*^{86} spermatocytes expressing GFP-tagged clathrin. Scale bar = 5μm.

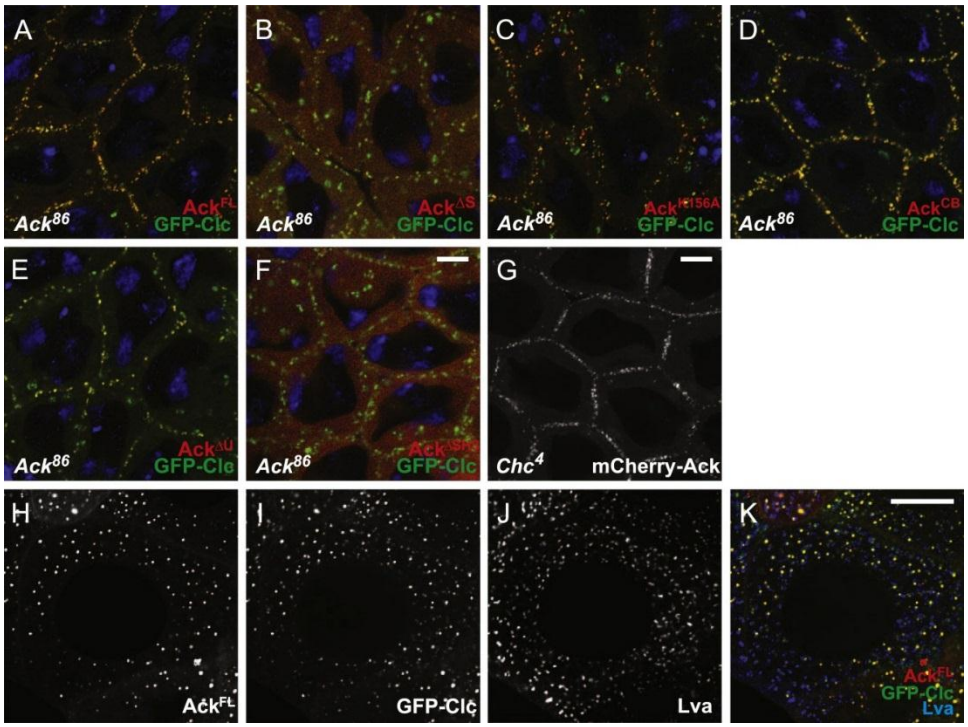

Figure 5 Ack localization requires SAM and SH3. (A-F) Laser scanning confocal micrographs of *Ack*^{86}**;** *β2Tub-GFP-Clc/+* spermatocytes expressing *β2Tub-mCherry-Ack*^{FL} (A), *β2Tub-mCherry-Ack*$^{\Delta S}$ (B), *β2Tub-mCherry-Ack*^{K156A} (C), *β2Tub-mCherry-Ack*^{CB} (D), *β2Tub-mCherry-Ack*$^{\Delta U}$ (E), and *β2Tub-mCherry-Ack*$^{\Delta SH3}$ (F). Clathrin, Ack constructs, and DNA are shown in green, red, and blue, respectively. Scale bar = 5μm. (G) Laser confocal electron micrographs of *Chc*^{4}*/Y; β2Tub-mCherry-Ack*^{FL}*/+* spermatocytes. Scale bar = 5μm. (H-K) Confocal image of *Act5C-GAL4, UAS-GFP-Clc; UAS-mCherry-Ack*^{FL} salivary gland cells stained with α-Lva antibody (blue). Scale bar = 10μm.

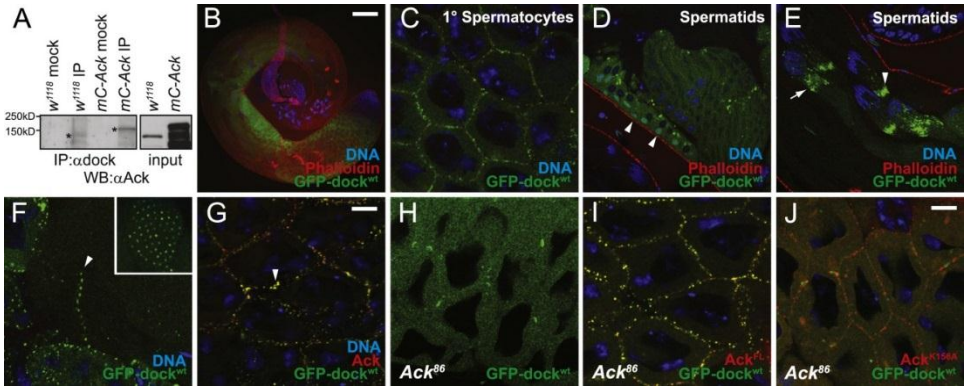

Figure 6. Dock localization requires Ack. (A) Endogenous Dock interacts with Ack in testes. Western analysis of w^{1118} and *β2Tub-mCherry-Ack*^{FL} testis lysates immunoprecipitated with α-Dock antibody and blotted with α-Ack antibody. A faint band corresponding to endogenous Ack is seen in w^{1118} IP lane, whereas a band corresponding to exogenously expressed mCherry-tagged Ack is seen in *β2Tub-mCherry-Ack*^{FL} lane (indicated by asterisks). No Ack band is detected in mock lanes, where α-Dock antibody is omitted during the immunoprecipitation. 3% of the lysates prior to IP are saved and loaded as input. (B-F) Confocal micrographs of *β2Tub-GFP-dock* testis stained with phalloidin (red) and Hoechst (blue). (B) A low magnification view showing that Dock distribution, like Ack, decreases significantly in elongating germ cell cysts. Scale bar = 100μm. (C-G) Dock localization in primary spermatocytes (C), pre-elongation spermatids (D), the nuclear ends of elongated spermatids (E), and the tail end of an elongated spermatid (F) is shown in green. Inset in (F) shows the cross-section of the ring-shaped structures at the tail end of an elongated germ cell cyst. (G) Confocal image of *β2Tub-GFP-dock/+; β2Tub-mCherry-Ack*^{FL}/+ spermatocytes. Hoechst-stained DNA is shown in blue. Scale bar = 5μm. (H-J) Confocal micrographs of *Ack*^{86} spermatocytes expressing *β2Tub-GFP-dock* (H), *β2Tub-GFP-dock* and *β2Tub-mCherry-Ack*^{FL} (I), and *β2Tub-GFP-dock* and *β2Tub-mCherry-Ack*^{K156A} (J). Scale bar = 5μm.

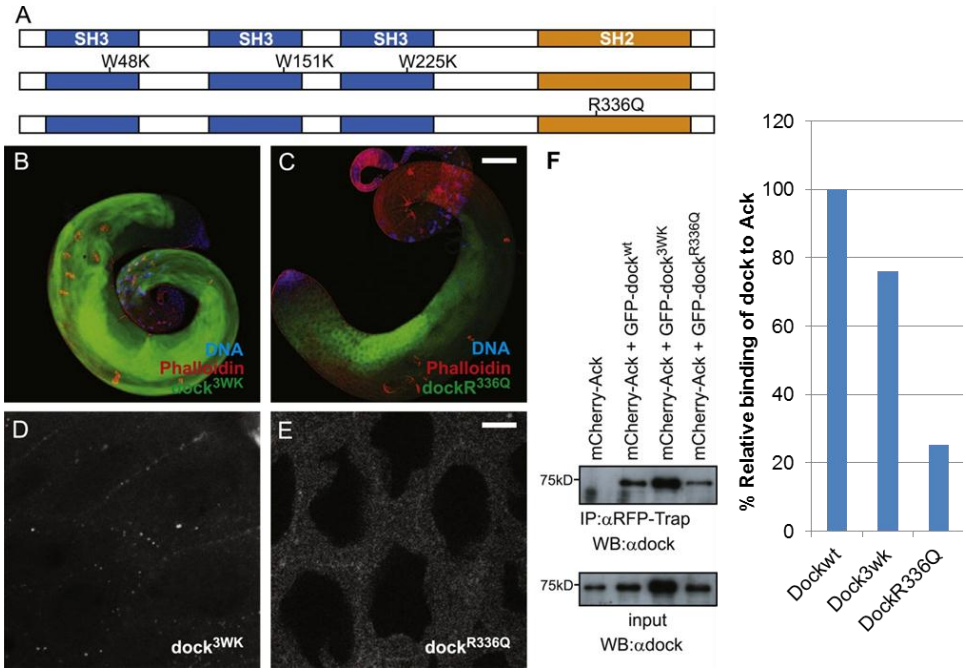

Figure 7. Dock localization requires the SH2 domain. (A) A schematic representation of *dock* constructs with the SH3 and SH2 domains indicated by blue and orange boxes, respectively. (B-C) Fluorescent micrographs of *β2Tub-GFP-dock*^{3WK} (B) and *β2Tub-GFP-dock*^{R336Q} (C) testes stained with phalloidin (red) and Hoechst (blue). Scale bar = 100μm. (D-E) Laser scanning confocal micrographs of *β2Tub-GFP-dock*^{3WK} (D) and *β2Tub-GFP-dock*^{R336Q} (E) spermatocytes. Scale bar = 5μm. (F) Western analysis of *w*^{1118} and *β2Tub-mCherry-Ack*^{FL} testis lysates immunoprecipitated with RFP-Trap beads and blotted with α-Dock antibody. While similar levels of tagged Dock proteins are seen in *β2Tub-GFP-dock*^{wt} and *β2Tub-GFP-dock*^{R336Q} input, less Dock^{R336Q} is seen in the IP lane. No GFP-dock is present in the IP with *β2Tub-mCherry-Ack*^{FL} lysate, although a non-specific band migrating around 75kD is detected in the input (also detected in *w*^{1118} lysate, not shown) by α-Dock antibody. 3% of the lysates prior to IP are saved and loaded as input.

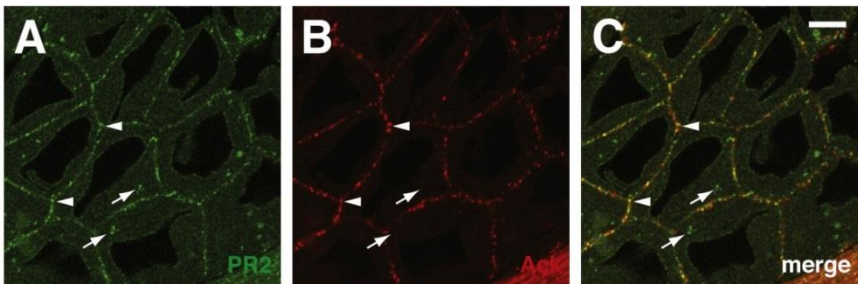

Figure 8. Exogenously expressed Ack and PR2 show few overlaps in spermatocytes. (A-C) Laser scanning confocal micrographs of spermatocytes expressing GFP-PR2 (A) and mCherry-Ack (B). PR2 and Ack both appear as vesicular structures around the cell periphery and show occasional colocalizations (arrowheads). However, PR2, but not Ack seems to associate more with internal structures (arrows). Scale bar = 5μm.

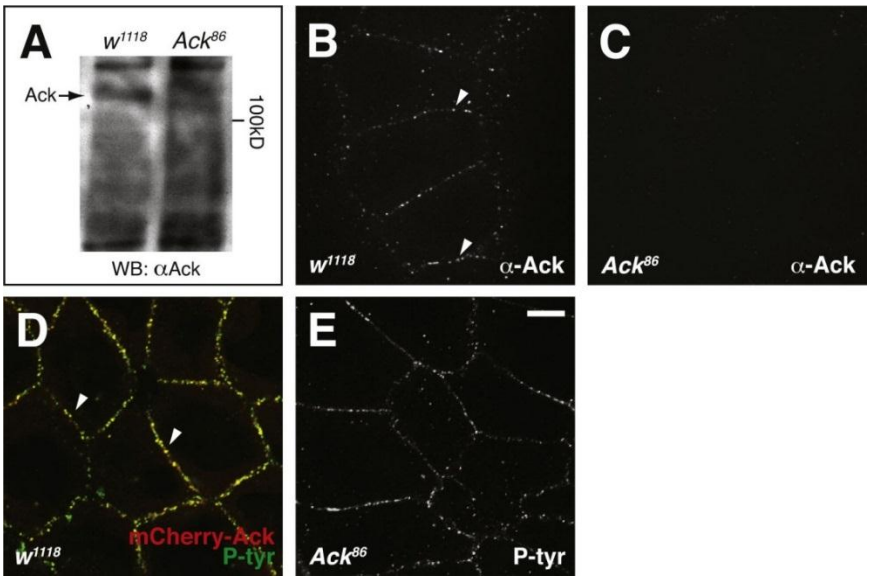

Figure 9. Endogenous Ack are seen as vesicular structures around cell periphery. (A) Western analysis of testis extracts probed with the rabbit polyclonal α-Ack antibody used in panels B and C. A band corresponding to the size of Ack (118.4kD, arrow) is seen in w^{1118} control, but not in Ack^{86} lane. (B-C) Spinning disc confocal micrographs of w^{1118} (B) and Ack^{86} (C) spermatocytes stained with the rabbit polyclonal α-Ack antibody. Similar to fluorescently tagged Ack, endogenous Ack localizes to vesicular structures around the cell periphery (arrowheads). (D-E) Confocal images of *β2Tub-mCherry-*Ack^{FL} (D) and Ack^{86} (E) spermatocytes stained with 4G10 α-phosphotyrosine antibody (green). Scale bar = 5μm.

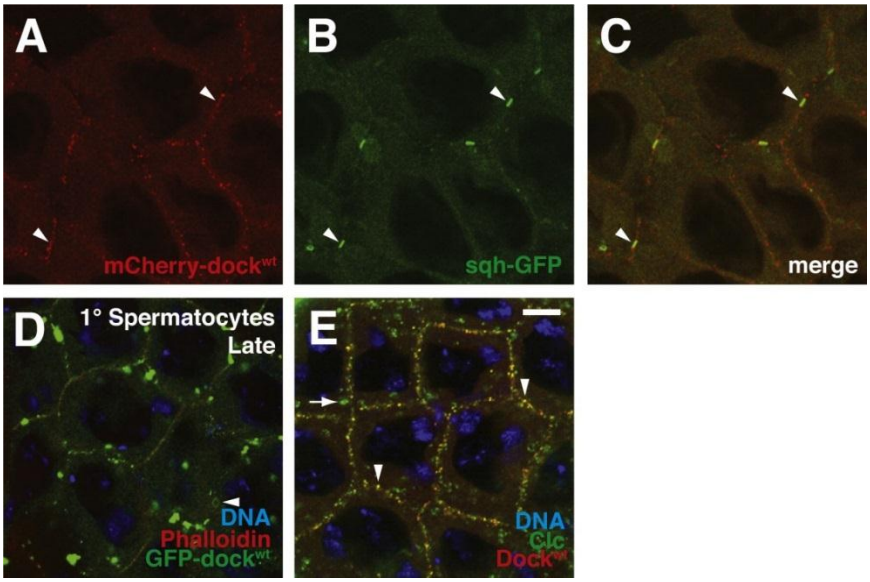

Figure 10. Dock localizes to the ring canals in spermatocytes. (A-C) Laser scanning confocal micrographs of spermatocytes expressing mCherry-dock (A) and sqh-GFP (B). Sqh (spaghetti squash), the myosin regulatory light chain, labels the contractile rings (arrowheads). (D) GFP-dock localization in late primary spermatocytes. Dock at a ring canal is indicated by an arrowhead. (E) Confocal image of *β2Tub-GFP-Clc/+; β2Tub-mCherry-dock^{wt}/+* spermatocytes. Hoechst-stained DNA is shown in blue. Similar to Ack, Dock colocalizes with clathrin around the cell periphery (arrowheads), but not with the internal clathrin-positive structures (arrows). Scale bar = 5μm.

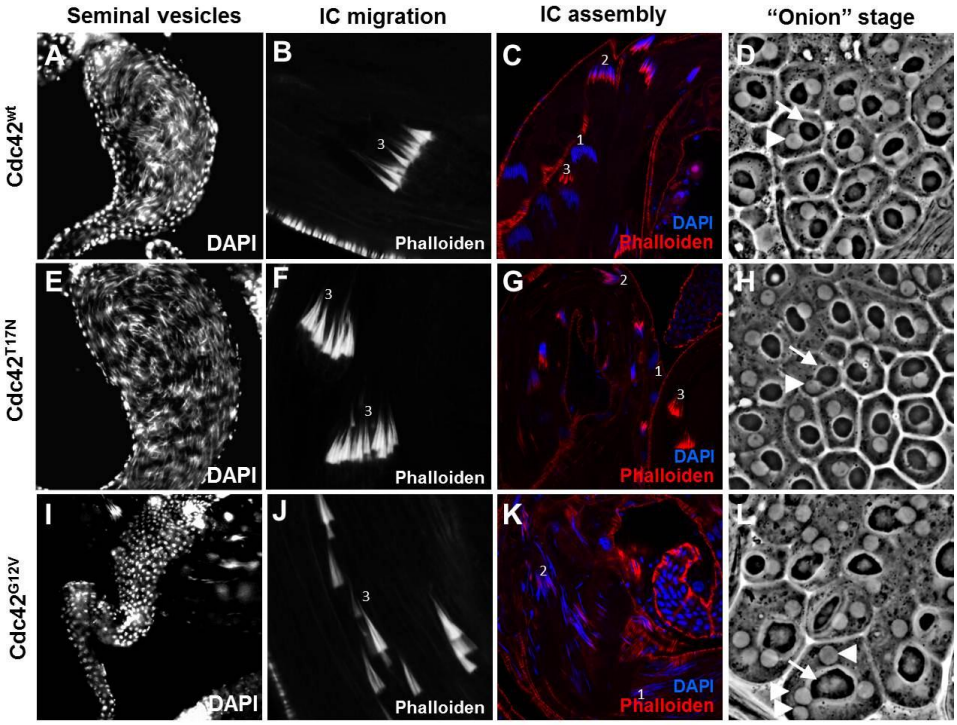

Figure 11. Over-expression of activated Cdc42 causes Cytokinesis defect: (A,E,I) Spinning disk confocal micrographs of Drosophila seminal vesicles, where DAPI was used to label sperm nuclei. Seminal vesicles are full with mature sperm in $Cdc42^{wt}$ (A) and $Cdc42^{T17N}$ (E), but few present in in $Cdc42^{G12V}$ (notice the collapsed empty seminal vesicles). (B,F,J) Laser confocal micrographs of migrating ICs(3) labelled by Phalloiden (filamentous actin) during individualization. ICs move in synchrony in $Cdc42^{wt}$ (B) and $Cdc42^{T17N}$ (F) but are scattered in $Cdc42^{G12V}$ indicating abnormal individualization. (C,G,K) Laser Confocal micrographs of elongated cysts with nuclei before (1) and during IC Assembly (2). DAPI (blue) labels spermatids' nuclei, Phalloiden (Red) labels ICs. Scattered pre assembly nuclei in $Cdc42^{G12V}$ (K) in comparison to bundled nuclei in $Cdc42^{wt}$ (C) and $Cdc42^{T17N}$(G). (D,H,L) Phase images of round spermatids at anion stage (64 cell stage). Dark circle (arrow) represents one mitochondrial body derivative, while one white circle (arrow head) represents one nucleus. Normal cytokinesis is observed in $Cdc42^{wt}$ (D) and $Cdc42^{T17N}$ (H) as one nucleus associates with one mitochondria. Cytokinesis is defective in $Cdc42^{G12V}$ since multiple nuclei associate with a singular mitochondrial body derivative (L).

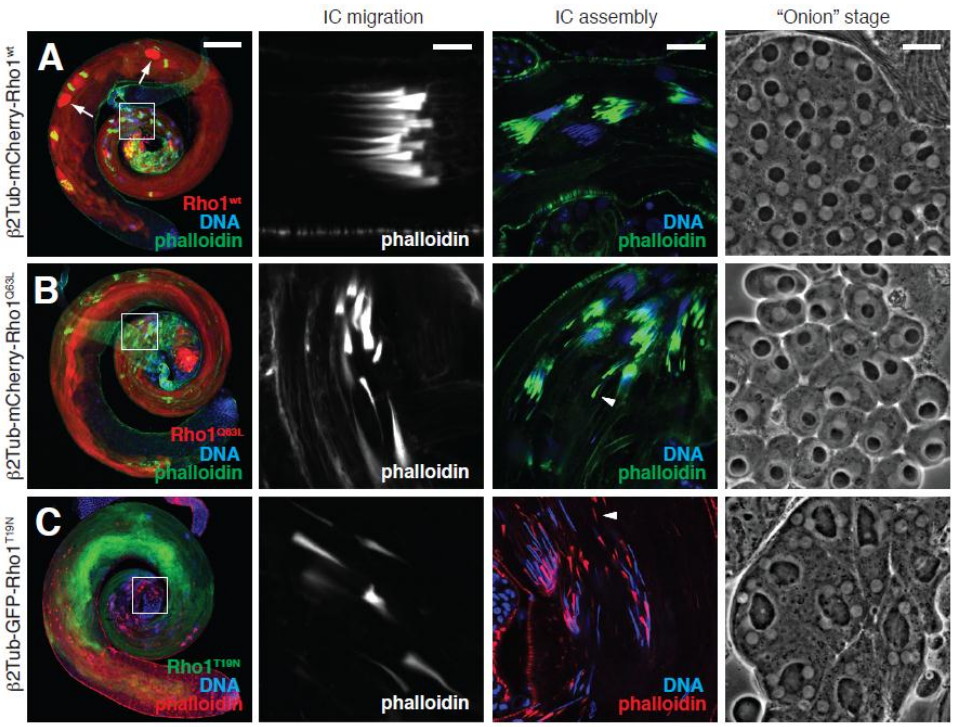

Figure 12. Over-expression of dominant negative dRho1 causes Cytokinesis defect: (A) Testis over-expressing mCherry tagged wild type Rho1 ($Rho1^{wt}$) have normal individualization (bundled ICs), normal elongation (bundled nuclei), and no cytokinesis defect (1 nucleus associates with mitochondrial body derivative at onion stage). (B) Over-expression of dominant active Rho1 ($Rho1^{Q63L}$) has some individualization defects (some scattered ICs), minor problems in elongation (nuclei show normal bundling), and no cytokinesis defects. (C) Over-expression of dominant negative ($Rho1^{T19N}$) shows abnormal individualization (scattered ICs), abnormal elongation (scattered nuclei) and strong cytokinesis defect (most mitochondrial bodies associate with four nuclei).

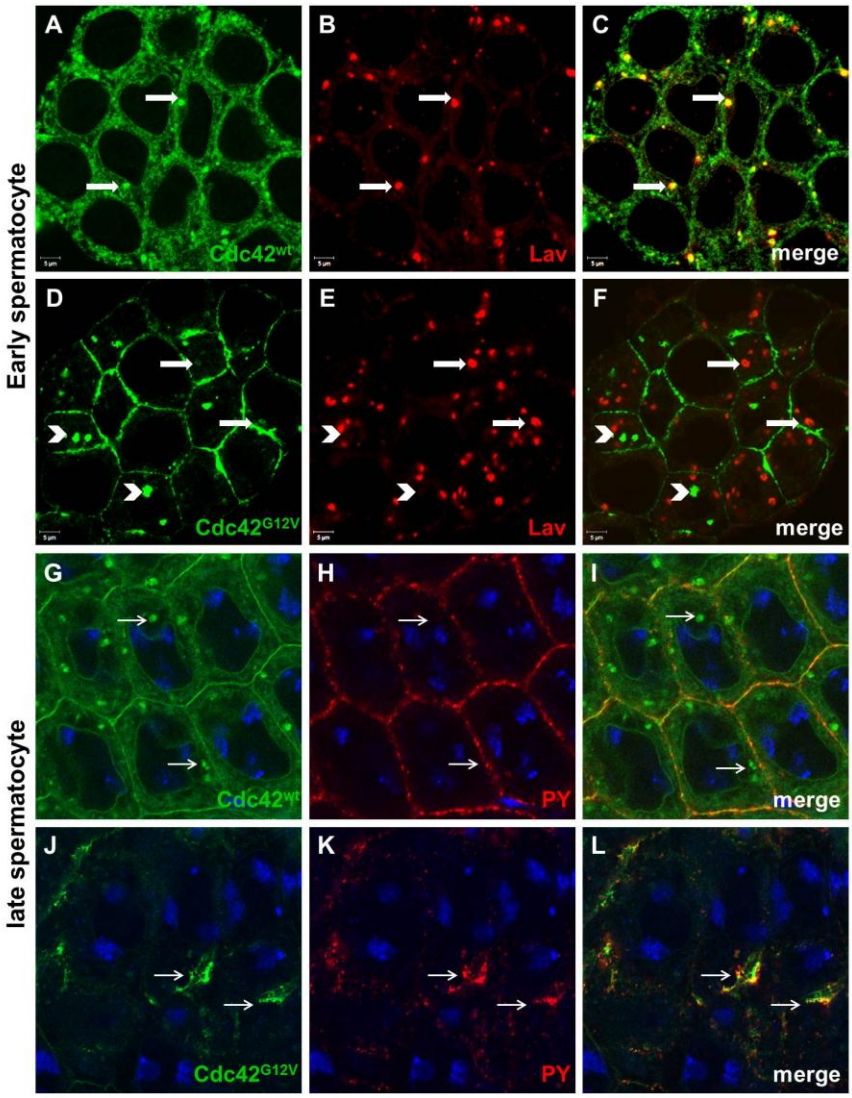

Figure 13. Activation of Cdc42 alters its subcellular localization: (A-L) Electron micrographs of early (A-F) and late (G-L) spermatocytes expressing either $Cdc42^{wt}$ or $Cdc42^{G12V}$ and stained with either αlava lamp (Golgi marker) or αG410 (PY). (A-C) $Cdc42^{wt}$ (Green) localizes in the cytoplasm and in puncta positive for the Golgi marker lava lamp (Red). (D-F) $Cdc42^{G12V}$ localizes in large structures that are lava lamp negative. It is also heavily present around cell periphery. (G-I) At late spermatocyte stage $Cdc42^{wt}$ is still present at Golgi but it is not rich in PY as indicated by G410 staining (Red). $Cdc42^{wt}$ is now also present around cell periphery. (J-L) At late spermatocyte stage, $Cdc42^{G12V}$ localizes to aberrant structures around cell periphery (arrows). These structures are highly rich in PY.

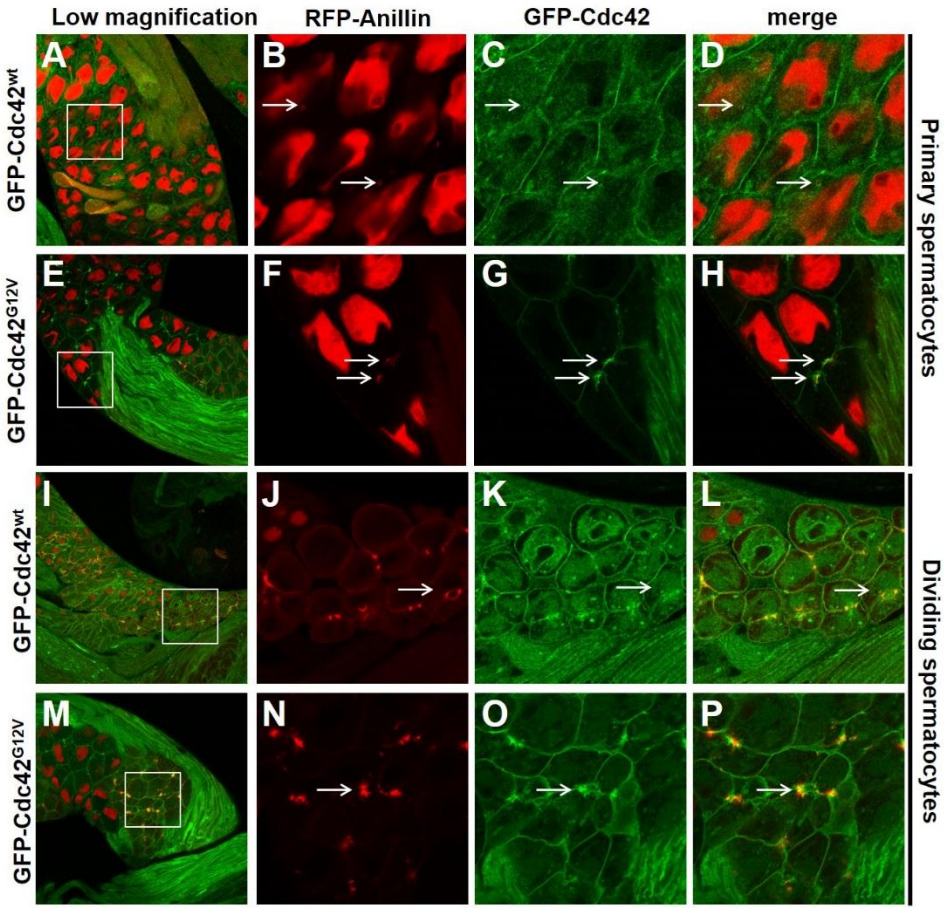

Figure 14. Activated Cdc42 Disrupts contractile ring: (A-P) laser confocal images of testis expressing anillin (red) with either $Cdc42^{wt}$ (Green) or $Cdc42^{G12V}$ (Green). Anillin labels ring canals at primary spermatocytes and contractile ring during cytokinesis. Low magnification image (A) of testis expressing anillin and $Cdc42^{wt}$. Higher magnification images of the boxed region where arrows indicate intact small ring canals between cells at early spermatocyte stage (B) with some $Cdc42^{wt}$ co-localization (C-D). Low magnification image (E) of testis expressing anillin and $Cdc42^{G12V}$. Higher magnification images of the boxed region where arrows indicate disrupted ring canals between cells at early spermatocyte stage (F) with $Cdc42^{G12V}$ accumulating in the vicinity of ring canals (G-H). Low magnification image (I) of testis expressing anillin and $Cdc42^{wt}$. Higher magnification images of the boxed region where arrows indicate intact contractile rings between dividing spermatocytes (J) with some $Cdc42^{wt}$ present at constriction sites(K-L). Low magnification image (M) of testis expressing anillin and $Cdc42^{G12V}$. Higher magnification images of the boxed region where arrows indicate disrupted contractile rings between dividing spermatocytes (N) with $Cdc42^{G12V}$ localizing in the vicinity of the contractile rings (O-P).

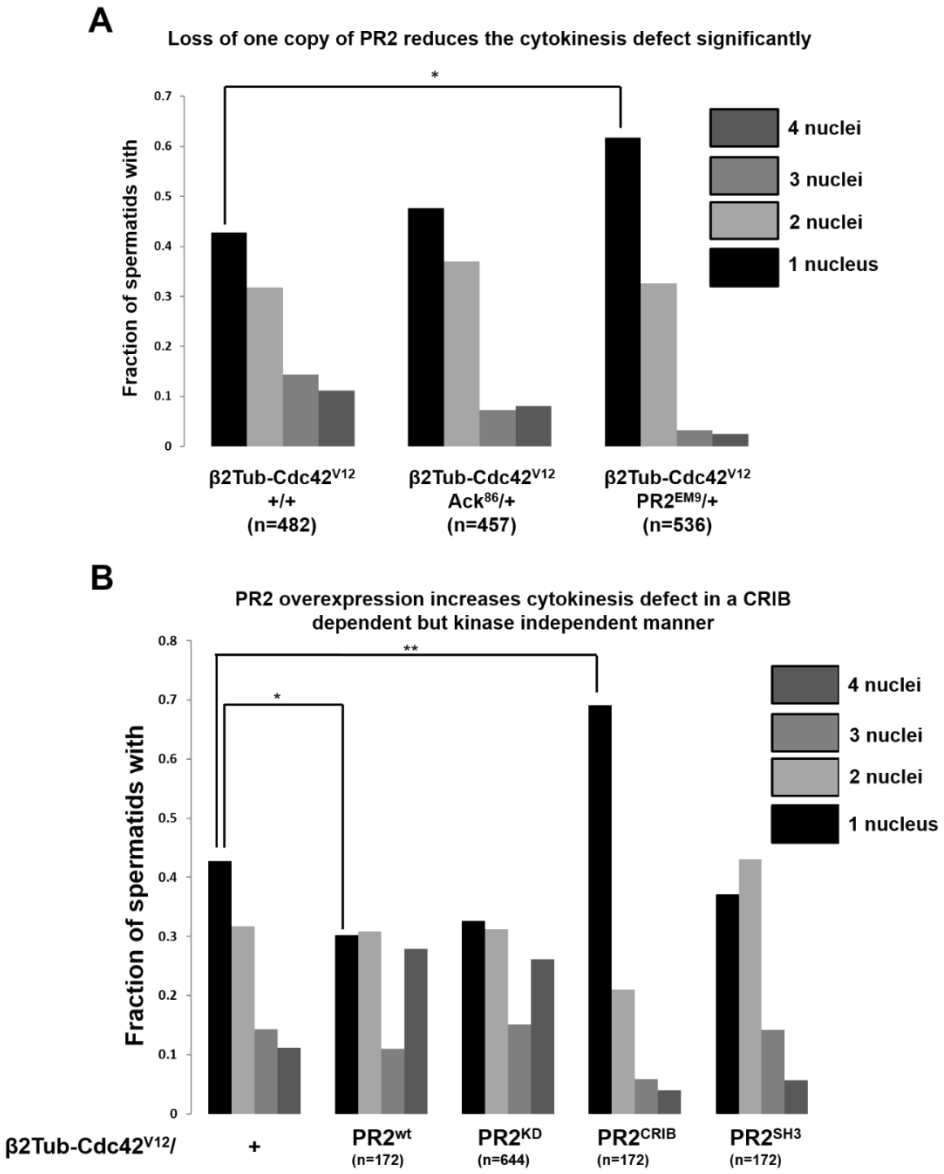

Figure 15. PR2 loss of function reduces the cytokinesis defect caused by Cdc42^{G12V}: (A-B) Bar graphs quantifying fraction of spermatids with one, two, three or four nuclei per one mitochondrial body caused by Cdc42^{G12V} over-expression in germline cells. (A) While the removal on one copy of Ack gene in testis expressing Cdc42^{G12V} doesn't significantly alter the number of round spermatids with cytokinesis defect compared to Cdc42^{G12V} alone, the removal of PR2 reduces the cytokinesis defect significantly. (B) The over expression of PR^{wt} and PR2^{KD} but not PR2^{SH3} significantly increase the cytokinesis defect caused by Cdc42^{G12V}. On the Contrary, the expression of PR2^{CRIB} significantly reduces the cytokinesis defect caused by Cdc42^{G12V}. (n= the number of round spermatids counted. * indicates p<0.01 while ** indicates p<0.001 Significance has beencalculated using a student T test).

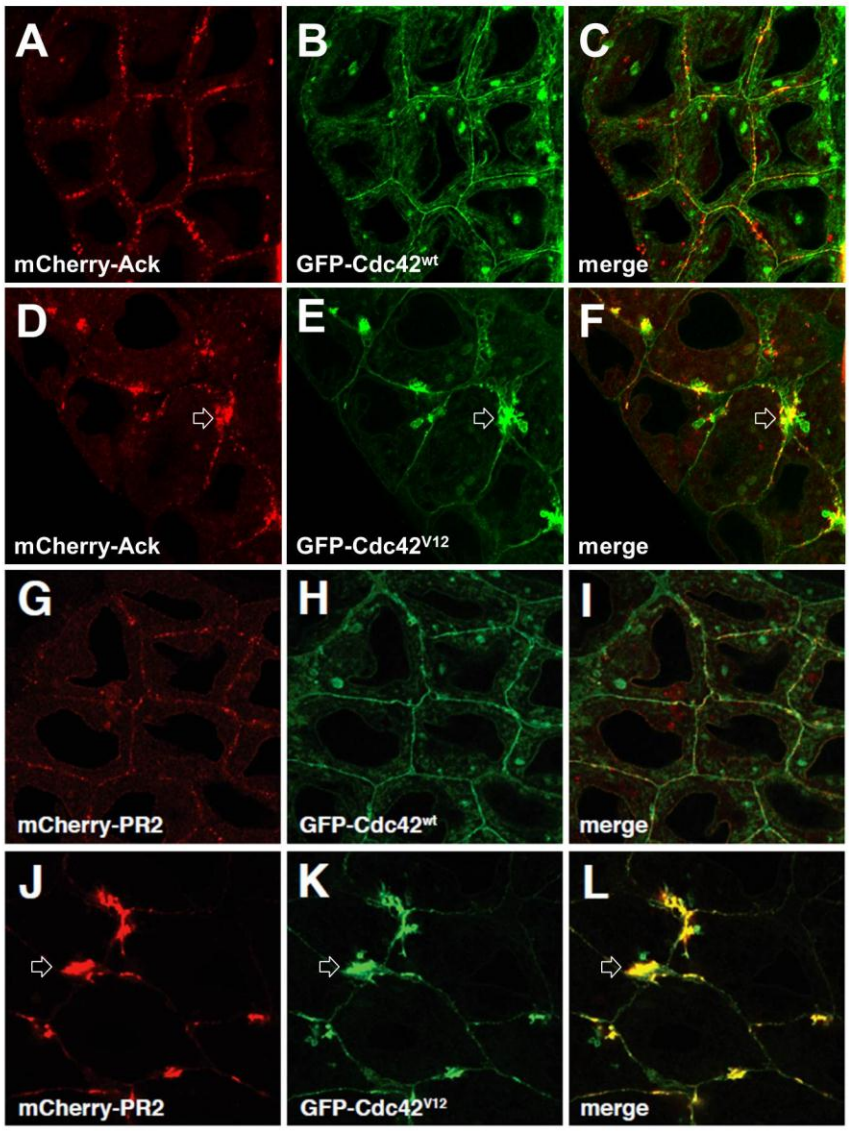

Figure 16. Cdc42^{G12V} alters the localization of Ack and PR2: (A-L) Laser electron micrographs of late 16 cell stage spermatocytes expressing or *β2Tub-mCherry-Ack*^{FL}or *β2Tub*-mCherry-PR2^{FL} with either *β2Tub-GFP-Cdc42*^{wt} or *β2Tub-GFP*-Cdc42^{G12V}. mCherry-Ack (A) and mCherry-PR2 (G) both localize mostly in puncta around cell periphery. These puncta localize poorly with GFP-Cdc42^{wt} (B-C,H-I). In GFP-Cdc42^{G12V} background, the localization of Both Ack (D) and PR2's (J) in puncta around cell periphery is mostly lost. Ack and PR are now present in the vicinity of activated Cdc42 at the site of ring canals (E-F, K-L).

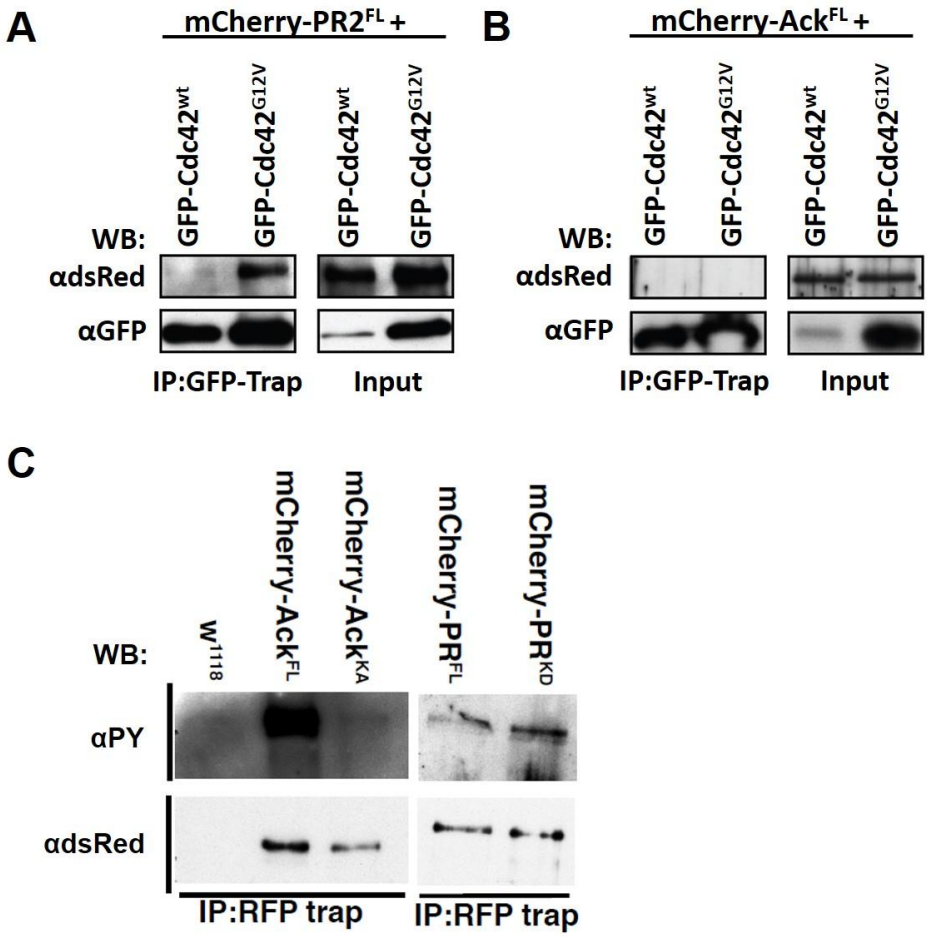

Figure 17. PR2 is pulled down in complex with Cdc42^{G12V}: (A-B) Western analysis of testis lysates co-expressing *β2Tub*-mCherry-PR2^{FL} or *β2Tub-mCherry-Ack^{FL}* with either *β2Tub-GFP-Cdc42^{wt}* or *β2Tub-GFP*-Cdc42^{G12V} immunoprecipitated with α-GFP trap and blotted with α-dsRed or α-GFP antibodies. 3% of the lysates were saved and run as input. A strong band corresponding to PR2 is present GFP-Cdc42^{G12V} IP but not GFP-Cdc42^{wt} (A). No bands corresponding to Ack were detected with either GFP-Cdc42^{wt} or GFP--Cdc42^{G12V} IPs. (C) Western analysis of w^{1118} testis lysates or testis expressing *β2Tub*-mCherry-PR2^{FL}, *β2Tub*-mCherry-PR2^{KD}, *β2Tub-mCherry-Ack^{FL}, or β2Tub-mCherry-Ack^{KD}*. mCherry-Ack or mCherry-PR2 were immunoprecipitated using α-RFP trap and blotted with αPY or αdsRed (loading control). Thick band observed in *β2Tub-mCherry-Ack^{FL}* compared to a much fainter one in *β2Tub-mCherry-Ack^{KD}*. Similar band intensity observed in *β2Tub*-mCherry-PR2^{FL} compared *β2Tub*-mCherry-PR2^{KD}.

REFERENCES

REFERENCES

Arama, E., Agapite, J., Steller, H., 2003. Caspase activity and a specific cytochrome C are required for sperm differentiation in Drosophila. Dev Cell. 4**,** 687-97.

Blumer, N., Schreiter, K., Hempel, L., Santel, A., Hollmann, M., Schafer, M. A., Renkawitz-Pohl, R., 2002. A new translational repression element and unusual transcriptional control regulate expression of don juan during Drosophila spermatogenesis. Mech Dev. 110**,** 97-112.

Boxall, A.R., & Lancaster, B. (2009). Tyrosine kinases and synaptic transmission. European Journal of Neuroscience, 10(1), 2-7.

Burgess, J., Jauregui, M., Tan, J., Rollins, J., Lallet, S., Leventis, P. A., Boulianne, G. L., Chang, H. C., Le Borgne, R., Kramer, H., Brill, J. A., 2011. AP-1 and clathrin are essential for secretory granule biogenesis in Drosophila. Mol Biol Cell. 22**,** 2094-105.

Cagan, R. L., Kramer, H., Hart, A. C., Zipursky, S. L., 1992. The bride of sevenless and sevenless interaction: internalization of a transmembrane ligand. Cell. 69**,** 393-9.

Chan, W., Tian, R., Lee, Y. F., Sit, S. T., Lim, L., Manser, E., 2009. Down-regulation of active ACK1 is mediated by association with the E3 ubiquitin ligase Nedd4-2. J Biol Chem. 284**,** 8185-94.

Clemens, J. C., Ursuliak, Z., Clemens, K. K., Price, J. V., Dixon, J. E., 1996. A Drosophila protein-tyrosine phosphatase associates with an adapter protein required for axonal guidance. J Biol Chem. 271**,** 17002-5.

Clemens, J. C., Worby, C. A., Simonson-Leff, N., Muda, M., Maehama, T., Hemmings, B. A., Dixon, J. E., 2000. Use of double-stranded RNA interference in Drosophila cell lines to dissect signal transduction pathways. Proc Natl Acad Sci U S A. 97**,** 6499-503.

Desai, C. J., Garrity, P. A., Keshishian, H., Zipursky, S. L., Zinn, K., 1999. The Drosophila SH2-SH3 adapter protein Dock is expressed in embryonic axons and facilitates synapse formation by the RP3 motoneuron. Development. 126, 1527-35.

Eisenmann, K. M., McCarthy, J. B., Simpson, M. A., Keely, P. J., Guan, J. L., Tachibana, K., Lim, L., Manser, E., Furcht, L. T., Iida, J., 1999. Melanoma chondroitin sulphate proteoglycan regulates cell spreading through Cdc42, Ack-1 and p130cas. Nat Cell Biol. 1, 507-13.

Eckhart, W., Hutchinson, M.A., & Hunter, T. (1979). An activity phosphorylating tyrosine in polyoma T antigen immunoprecipitates. Cell, 18, 925-933.

Fabrizio, J. J., Hime, G., Lemmon, S. K., Bazinet, C., 1998. Genetic dissection of sperm individualization in Drosophila melanogaster. Development. 125, 1833-43.

Fares, H., Peifer, M. and Pringle, J. R. (1995). Localization and possible functions of Drosophila septins. Mol. Biol. Cell 6, 1843-1859.

Farkas, R. M., Giansanti, M. G., Gatti, M., Fuller, M. T., 2003. The Drosophila Cog5 homologue is required for cytokinesis, cell elongation, and assembly of specialized Golgi architecture during spermatogenesis. Mol Biol Cell. 14, 190-200.

Field, C. M. and Alberts, B. M. (1995). Anillin, a contractile ring protein that cycles from the nucleus to the cell cortex. J. Cell Biol. 131, 165-78.

Field, C. M., Al-Awar, O., Rosenblatt, J., Wong, M. L., Alberts, B. and Mitchison, T. J. (1996). A purified Drosophila septin complex forms filaments and exhibits GTPase activity. J. Cell Biol. 133, 605-616.

Galisteo, M. L., Yang, Y., Urena, J., Schlessinger, J., 2006. Activation of the nonreceptor protein tyrosine kinase Ack by multiple extracellular stimuli. Proc Natl Acad Sci U S A. 103, 9796-801.

Garrity, P. A., Rao, Y., Salecker, I., McGlade, J., Pawson, T., Zipursky, S. L., 1996. Drosophila photoreceptor axon guidance and targeting requires the dreadlocks SH2/SH3 adapter protein. Cell. 85, 639-50.

Gonczy, P., DiNardo, S., 1996. The germ line regulates somatic cyst cell proliferation and fate during Drosophila spermatogenesis. Development. 122, 2437-47.

Grovdal, L. M., Johannessen, L. E., Rodland, M. S., Madshus, I. H., Stang, E., 2008. Dysregulation of Ack1 inhibits down-regulation of the EGF receptor. Exp Cell Res. 314, 1292-300.

Hardy, R. W., Tokuyasu, K. T., Lindsley, D. L., Garavito, M., 1979. The germinal proliferation center in the testis of Drosophila melanogaster. J Ultrastruct Res. 69, 180-90.

Hime, G. R., Brill, J. A., Fuller, M. T., 1996. Assembly of ring canals in the male germ line from structural components of the contractile ring. J Cell Sci. 109 (Pt 12), 2779-88.

Hirst, J., Sahlender, D. A., Choma, M., Sinka, R., Harbour, M. E., Parkinson, M., Robinson, M. S., 2009. Spatial and functional relationship of GGAs and AP-1 in Drosophila and HeLa cells. Traffic. 10, 1696-710.

Hoare, S., Hoare, K., Reinhard, M. K., Lee, Y. J., Oh, S. P., May, W. S., Jr., 2008. Tnk1/Kos1 knockout mice develop spontaneous tumors. Cancer Res. 68, 8723-32.

Hopper, N. A., Lee, J., Sternberg, P. W., 2000. ARK-1 inhibits EGFR signaling in C. elegans. Mol Cell. 6, 65-75.

Huh, J. R., Vernooy, S. Y., Yu, H., Yan, N., Shi, Y., Guo, M., Hay, B. A., 2004. Multiple apoptotic caspase cascades are required in nonapoptotic roles for Drosophila spermatid individualization. PLoS Biol. 2, E15.

Hunter, T. (2009). Tyrosine phosphorylation: thirty years and counting. Current Opinion in Cell Biology, 21(2), 140-146.

Isakoff, S.J., Cardozo, T., Andreev, J., Li, Z., Ferguson, K.M., Abagyan, R., Lemmon, M.A., Aronheim, A., & Skolnik, E.Y. (1998). The EMBO Journal, 17(18), 5374-5387.

Jose, A. M., Kim, Y. A., Leal-Ekman, S., Hunter, C. P., 2012. Conserved tyrosine kinase promotes the import of silencing RNA into Caenorhabditis elegans cells. Proc Natl Acad Sci U S A. 109, 14520-5.

Kemphues, K. J., Kaufman, T. C., Raff, R. A., Raff, E. C., 1982. The testis-specific beta-tubulin subunit in Drosophila melanogaster has multiple functions in spermatogenesis. Cell. 31, 655-70.

Kramer, H., Phistry, M., 1996. Mutations in the Drosophila hook gene inhibit endocytosis of the boss transmembrane ligand into multivesicular bodies. J Cell Biol. 133, 1205-15.

Lew, D.J., & Kornbluth, S. (1996). Regulatory roles of cyclin dependent kinase phosphorylation in cell cycle control. Current Opinion in Cell Biology, 8(6), 795-804.

Lin, Q., Wang, J., Childress, C., Sudol, M., Carey, D. J., Yang, W., 2010. HECT E3 ubiquitin ligase Nedd4-1 ubiquitinates ACK and regulates epidermal growth factor (EGF)-induced degradation of EGF receptor and ACK. Mol Cell Biol. 30**,** 1541-54.

Lin, Q., Wang, J., Childress, C., Yang, W., 2012. The activation mechanism of ACK1 (activated Cdc42-associated tyrosine kinase 1). Biochem J. 445**,** 255-64.

Lin, T.H., Yurochko, A., Kornberg, L., Morris, J., Walker, J.J., Haskill, S., & Juliano, R.L. (1994). The role of protein tyrosine phosphorylation in integrin-mediated gene induction in monocytes. The Journal of Cell Biology, 126(6), 1585-1593.

Lindsley, D. L., Tokuyasu, K. T., Spermatogenesis. In: M. Ashburner, T. R. F. Wright, Eds.), The Genetics and Biology of Drosophila, Vol. 2. New York: Academic Press, 1980, pp. 225-294.

Mahajan, K., Coppola, D., Challa, S., Fang, B., Chen, Y. A., Zhu, W., Lopez, A. S., Koomen, J., Engelman, R. W., Rivera, C., Muraoka-Cook, R. S., Cheng, J. Q., Schonbrunn, E., Sebti, S. M., Earp, H. S., Mahajan, N. P., 2010. Ack1 mediated AKT/PKB tyrosine 176 phosphorylation regulates its activation. PLoS One. 5**,** e9646.

Mahajan, N. P., Liu, Y., Majumder, S., Warren, M. R., Parker, C. E., Mohler, J. L., Earp, H. S., Whang, Y. E., 2007. Activated Cdc42-associated kinase Ack1 promotes prostate cancer progression via androgen receptor tyrosine phosphorylation. Proc Natl Acad Sci U S A. 104**,** 8438-43.

Mahajan, N. P., Whang, Y. E., Mohler, J. L., Earp, H. S., 2005. Activated tyrosine kinase Ack1 promotes prostate tumorigenesis: role of Ack1 in polyubiquitination of tumor suppressor Wwox. Cancer Res. 65**,** 10514-23.

Manser, E., Leung, T., Salihuddin, H., Tan, L., Lim, L., 1993. A non-receptor tyrosine kinase that inhibits the GTPase activity of p21cdc42. Nature. 363**,** 364-7.

Neufeld, T. P. and Rubin, G. R. (1994). The Drosophila peanut gene is required for cytokinesis and encodes a protein similar to yeast putative bud neck filament proteins. Cell 77, 371-379.

Olsen J.V., Blagoev, B., Gnad, F., Macek, B., Kumar, C., Mortensen, P., & Mann, M. (2006). Global, in vivo, and site-specific phosphorylation dynamics in signaling networks. Cell, 127, 635–648.

Pawson, T. (2004). Specificity in signal transduction: from phosphotyrosine-SH2 domain interactions to complex cellular systems. Cell, 116(2), 191-203.

Peralta, S., Gomez, Y., Gonzalez-Gaitan, M. A., Moya, F., Vinos, J., 2009. Notch down-regulation by endocytosis is essential for pigment cell determination and survival in the Drosophila retina. Mech Dev. 126**,** 256-69.

Prieto-Echague, V., Gucwa, A., Brown, D. A., Miller, W. T., 2010a. Regulation of Ack1 localization and activity by the amino-terminal SAM domain. BMC Biochem. 11**,** 42.

Prieto-Echague, V., Gucwa, A., Craddock, B. P., Brown, D. A., Miller, W. T., 2010b. Cancer-associated mutations activate the nonreceptor tyrosine kinase Ack1. J Biol Chem. 285**,** 10605-15.

Rao, Y., Zipursky, S. L., 1998. Domain requirements for the Dock adapter protein in growth- cone signaling. Proc Natl Acad Sci U S A. 95**,** 2077-82.

Rivero-Lezcano, O. M., Marcilla, A., Sameshima, J. H., Robbins, K. C., 1995. Wiskott-Aldrich syndrome protein physically associates with Nck through Src homology 3 domains. Mol Cell Biol. 15**,** 5725-31.

Robinett, C. C., Giansanti, M. G., Gatti, M., Fuller, M. T., 2009. TRAPPII is required for cleavage furrow ingression and localization of Rab11 in dividing male meiotic cells of Drosophila. J Cell Sci. 122**,** 4526-34.

Rohatgi, R., Nollau, P., Ho, H. Y., Kirschner, M. W., Mayer, B. J., 2001. Nck and phosphatidylinositol 4,5-bisphosphate synergistically activate actin polymerization through the N-WASP-Arp2/3 pathway. J Biol Chem. 276**,** 26448-52.

Rotkopf, S., Hamberg, Y., Aigaki, T., Snapper, S. B., Shilo, B. Z., Schejter, E. D., 2011. The WASp-based actin polymerization machinery is required in somatic support cells for spermatid maturation and release. Development. 138**,** 2729-39.

Rubin, G. M., Spradling, A. C., 1982. Genetic transformation of Drosophila with transposable element vectors. Science. 218**,** 348-53.

Santel, A., Blumer, N., Kampfer, M., Renkawitz-Pohl, R., 1998. Flagellar mitochondrial association of the male-specific Don Juan protein in Drosophila spermatozoa. J Cell Sci. 111 (Pt 22), 3299-309.

Santel, A., Winhauer, T., Blumer, N., Renkawitz-Pohl, R., 1997. The Drosophila don juan (dj) gene encodes a novel sperm specific protein component characterized by an unusual domain of a repetitive amino acid motif. Mech Dev. 64, 19-30.

Schlessinger, J., & Ullrich, A. (1992). Growth factor signaling by receptor tyrosine kinases. Neuron, 9(3), 383-391.

Schoenherr, J. A., Drennan, J. M., Martinez, J. S., Chikka, M. R., Hall, M. C., Chang, H. C., Clemens, J. C., 2012. Drosophila activated Cdc42 kinase has an anti-apoptotic function. PLoS Genet. 8, e1002725.

Shen, F., Lin, Q., Gu, Y., Childress, C., Yang, W., 2007. Activated Cdc42-associated kinase 1 is a component of EGF receptor signaling complex and regulates EGF receptor degradation. Mol Biol Cell. 18, 732-42.

Shen, H., Ferguson, S. M., Dephoure, N., Park, R., Yang, Y., Volpicelli-Daley, L., Gygi, S., Schlessinger, J., De Camilli, P., 2011. Constitutive activated Cdc42-associated kinase (Ack) phosphorylation at arrested endocytic clathrin-coated pits of cells that lack dynamin. Mol Biol Cell. 22, 493-502.

Sisson, J. C., Field, C., Ventura, R., Royou, A., Sullivan, W., 2000. Lava lamp, a novel peripheral golgi protein, is required for Drosophila melanogaster cellularization. J Cell Biol. 151, 905-18.

Teo, M., Tan, L., Lim, L., Manser, E., 2001. The tyrosine kinase ACK1 associates with clathrin-coated vesicles through a binding motif shared by arrestin and other adaptors. J Biol Chem. 276, 18392-8.

Tokuyasu, K. T., Peacock, W. J., Hardy, R. W., 1972. Dynamics of spermiogenesis in Drosophila melanogaster. I. Individualization process. Z Zellforsch Mikrosk Anat. 124, 479-506.

Ushiro, H., & Cohen, S. (1980). Identification of phosphotyrosine as a product of epidermal growth factor-activated protein kinase in A-431 cell membranes. Journal of Biological Chemistry, 255, 8363-8365.

van der Horst, E. H., Degenhardt, Y. Y., Strelow, A., Slavin, A., Chinn, L., Orf, J., Rong, M., Li, S., See, L. H., Nguyen, K. Q., Hoey, T., Wesche, H., Powers, S., 2005. Metastatic properties and genomic amplification of the tyrosine kinase gene ACK1. Proc Natl Acad Sci U S A. 102, 15901-6.

Worby, C. A., Simonson-Leff, N., Clemens, J. C., Huddler, D., Jr., Muda, M., Dixon, J. E., 2002. Drosophila Ack targets its substrate, the sorting nexin DSH3PX1, to a protein complex involved in axonal guidance. J Biol Chem. 277**,** 9422-8.

Yang, W., Lin, Q., Guan, J. L., Cerione, R. A., 1999. Activation of the Cdc42-associated tyrosine kinase-2 (ACK-2) by cell adhesion via integrin beta1. J Biol Chem. 274**,** 8524-30.

Yang, W., Lo, C. G., Dispenza, T., Cerione, R. A., 2001. The Cdc42 target ACK2 directly interacts with clathrin and influences clathrin assembly. J Biol Chem. 276**,** 17468-73.

Yeow-Fong, L., Lim, L., Manser, E., 2005. SNX9 as an adaptor for linking synaptojanin-1 to the Cdc42 effector ACK1. FEBS Lett. 579**,** 5040-8.

Yokoyama, N., Miller, W. T., 2003. Biochemical properties of the Cdc42-associated tyrosine kinase ACK1. Substrate specificity, authphosphorylation, and interaction with Hck. J Biol Chem. 278**,** 47713-23.

Zahedi, B., Shen, W., Xu, X., Chen, X., Mahey, M., Harden, N., 2008. Leading edge-secreted Dpp cooperates with ACK-dependent signaling from the amnioserosa to regulate myosin levels during dorsal closure. Dev Dyn. 237**,** 2936-46.

Zhang, J., Schulze, K. L., Hiesinger, P. R., Suyama, K., Wang, S., Fish, M., Acar, M., Hoskins, R. A., Bellen, H. J., Scott, M. P., 2007. Thirty-one flavors of Drosophila rab proteins. Genetics. 176**,** 1307-22.

Zhou, X., Fabian, L., Bayraktar, J. L., Ding, H. M., Brill, J. A., Chang, H. C., 2011. Auxilin is required for formation of Golgi-derived clathrin-coated vesicles during Drosophila spermatogenesis. Development. 138**,** 1111-20

VITA

VITA

Abbas Abdallah
Department of Biological Sciences, Purdue University

Education
B.S., Biological sciences, 2008, Lebanese American University, Beirut, Lebanon
Ph.D., Cell and molecular Biology, 2014, Purdue University, West Lafayette, Indiana

Future direction
Post doctorate position at University of Massachusetts medical school with Dr. Fen-Biao Gao studying Frontotemporal Dementia.

Honors and Awards:
2012. Best oral presentation at the Biology Graduate Student Retreat.
2012. Graduate Student Summer 2012 Research Grant.$2800
2012. Member of the Golden Key honor society (upon invitation, top 15% of class)
2007. Invited to attend the Café Scientifique event held by the British council representing LAU. Beirut, Lebanon.
2006. LAU travel grant to attend the International Conference on Environment
2006. Penang, Malaysia. 2000$
2005-2008. Tuition scholarship (LAU) based on GPA. (About 7000$/year)
2005-2008.Honor list society throughout undergraduate degree at LAU.

Publications:

A. Abdallah, X. Zhou, C. Kim, K. Shah, C. Hogden, J. Schoenherr, J. Clemens, H. Chang. (2013). Activated Cdc42 kinase regulates Dock localization in male germ cells during Drosophila spermatogenesis. Developmental Biology

N. Yahia, **A. Abdallah**, A. Achkar, S, Rizk. (2010). Physical Activity, Smoking Practices, and Weight Status among Lebanese university students. International Journal of Health Research Vol 3(1), 21-29.

N. Yahia, A. Achkar, **A. Abdallah**, S, Rizk. (2008). Eating habits and obesity among Lebanese university students. Nutrition Journal 2008, 7:32